

Structure–Activity Relationship Studies of Novel Benzophenones Leading to the Discovery of a Potent, Next Generation HIV Nucleoside Reverse Transcriptase Inhibitor

Karen R. Romines,^{†,*} George A. Freeman,[†] Lee T. Schaller,[†] Jill R. Cowan,[†] Steve S. Gonzales,[†] Jeffrey H. Tidwell,[†] Clarence W. Andrews, III,[†] David K. Stammers,[‡] Richard J. Hazen,[†] Robert G. Ferris,[†] Steven A. Short,[†] Joseph H. Chan,[†] and Lawrence R. Boone[†]

GlaxoSmithKline Inc., Research Triangle Park, North Carolina 27709, and University of Oxford, Oxford, UK

Received July 14, 2005

Despite the progress of the past two decades, there is still considerable need for safe, efficacious drugs that target human immunodeficiency virus (HIV). This is particularly true for the growing number of patients infected with virus resistant to currently approved HIV drugs. Our high throughput screening effort identified a benzophenone template as a potential nonnucleoside reverse transcriptase inhibitor (NNRTI). This manuscript describes our extensive exploration of the benzophenone structure–activity relationships, which culminated in the identification of several compounds with very potent inhibition of both wild type and clinically relevant NNRTI-resistant mutant strains of HIV. These potent inhibitors include **70h** (GW678248), which has in vitro antiviral assay IC₅₀ values of 0.5 nM against wild-type HIV, 1 nM against the K103N mutant associated with clinical resistance to efavirenz, and 0.7 nM against the Y181C mutant associated with clinical resistance to nevirapine. Compound **70h** has also demonstrated relatively low clearance in intravenous pharmacokinetic studies in three species, and it is the active component of a drug candidate which has progressed to phase 2 clinical studies.

Introduction

The use of combination therapy, or highly active antiretroviral therapy (HAART), for treatment of human immunodeficiency virus (HIV) infection has dramatically impacted the disease. Diligent use of available anti-retroviral drugs can control an HIV infection for several years, and as a consequence, the death rate of HIV patients in the developed world fell dramatically in the mid to late 1990s. Nonnucleoside reverse transcriptase inhibitors (NNRTI's), including nevirapine and efavirenz, are proving to be important components of HAART. In particular, the use of efavirenz in combination with two nucleosides (e.g., lamivudine and zidovudine) is an excellent first-line therapy for HIV patients, and it has been used extensively in recent years.¹

As with all antiretroviral drugs developed to date, the use of the NNRTI's has led to the appearance of clinical resistance to this class of drugs. Unfortunately, the genetic barrier of all current NNRTI's is relatively low, and a single mutation can begin to reduce the susceptibility of virus to drug. Furthermore, cross resistance between the approved NNRTI's (efavirenz, nevirapine, and delavirdine) is quite common, and patients are generally forced to abandon the approved NNRTI's altogether once they have developed resistance to one of its members.^{2,3} To make the situation even worse, the appearance of drug-resistant virus is not limited to NNRTI-experienced patients. Recent studies indicate the number of newly infected patients with NNRTI-resistant virus is increasing.⁴ In one U.S. cohort which included antiretroviral naïve patients from 44 cities, 18% had decreased phenotypic sensitivity to at least one NNRTI, and one-third of these had decreased phenotypic sensitivity to all currently used NNRTI's.⁵

Efavirenz and nevirapine are the most widely used NNRTI's. Although resistance patterns in the presence of the multidrug

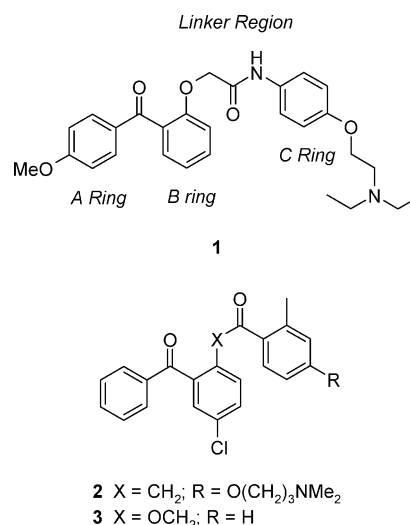


Figure 1. Initial benzophenone NNRTI lead structures.

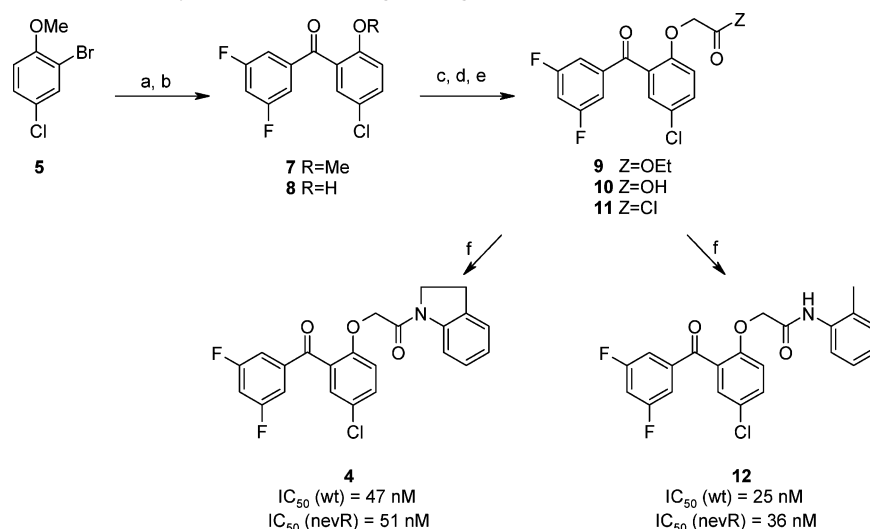
regimens of HIV care are complex, it's clear that each of these NNRTI's is associated with a single point mutation that triggers the development of clinical resistance. For efavirenz, it is the K103N mutation. For nevirapine, it is the Y181C mutation.² Consequently, these mutant viruses have been a focal point in our search for a next generation NNRTI.

Our efforts to discover an NNRTI efficacious against resistant viral strains originated in a high throughput screening effort which identified the benzophenone **1** (Figure 1).⁶ The initial optimization work for this template was published in 1995. The finding that resistant viruses readily generated in the presence of the leading analogue **2** were cross-resistant to nevirapine led to decreased interest in further optimization of the benzophenones at that time, and work in this compound series was briefly stopped. Because of the importance of this drug class, however, we turned our attention once more to the benzophenones in the late 1990s, as one of several potential templates for targeting

* Corresponding author. Phone: 919 483 4749. Fax: 919 315 2141. E-mail: Karen.r.romines@gsk.com.

[†] GlaxoSmithKline Inc.

[‡] University of Oxford.

Scheme 1. Synthesis of Conformationally Constrained C-Ring Analogues^a

^a (a) **5** to **7**: *n*BuLi, Et₂O, -78 °C; then 3,5-diFPhCON(OMe)Me (**6**), -78 °C to room temperature, 42%; (b) **7** to **8**: BBr₃, CH₂Cl₂, -78 °C to room temperature, 98%; (c) **8** to **9**: BrCH₂CO₂Et, K₂CO₃, acetone, reflux, 4 h, 100%; (d) **9** to **10**: LiOH, H₂O, EtOH, THF, rt, 3h, 81%; (e) **10** to **11**: (ClCO)₂, DMF, CH₂Cl₂, rt, 1 h; (f) amine, NaHCO₃, acetone, H₂O, rt, 2.5 h, 37–58%. IC₅₀ values were determined using an acute infection assay in MT4 cells. Wild type (wt) virus is the HIV-1 IIIB strain. The nevirapine resistant virus (nevR) contains the Y181C mutation.

resistant viruses. Guided by data from a panel of mutant viruses, we were able to transform this template into a series of compounds with potency against clinically relevant NNRTI-resistant viruses.⁷ This manuscript will describe the structure–activity relationships leading to the initial activity against mutant viruses, as well as the additional modifications which led to a dramatic increase in potency. We will also outline the data on drug development characteristics which differentiated very potent inhibitors, leading to the identification of **70h** (GW678248, see Table 4) as a promising next generation NNRTI.

Results and Discussion

The original optimization of **1** indicated that the carbonyl between the A- and B-rings was important for activity, and a methyl substituent ortho to the amide on the C-ring gave the molecule a measure of metabolic stability. On the C-ring, further substitution was best placed at the para position, but no beneficial substitution of the A-ring was identified.⁶

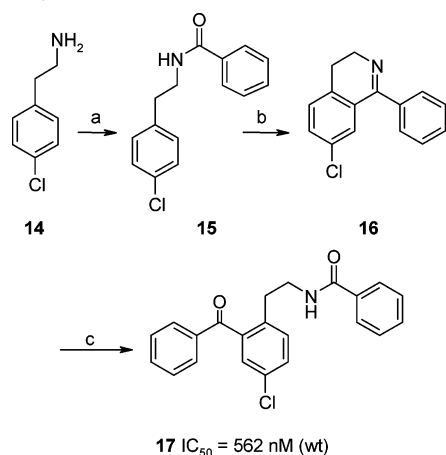
A crystal structure of the unsubstituted analogue **3** complexed with wild-type HIV reverse transcriptase was obtained by Stammers and colleagues,⁸ and this work confirmed that the benzophenone analogue occupied the nonnucleoside binding pocket. The X-ray crystal structure also indicated that space could be available for meta substitution in the A-ring and para substitution in the C-ring. Study of the structure led to the following hypotheses: (1) Meta substitution on the A-ring would reach into the hydrophobic region adjacent to the side chains of Y181 and Y188 and thus would require a polar aprotic and sterically small substituent, such as cyano (or a small nonpolar group at the expense of solubility). (2) The para position on the C-ring pointed directly into the exterior water through a rather small window in the protein surface. Para substitution could thus be used to add a water solubilizing group that could counter the lipophilic nature of the benzophenone scaffold. (3) The internal hydrogen bond between the benzophenone carbonyl and the amide NH could be maintained in the benzophenone:enzyme complex.

Modifications of the Linker Region and B-Ring. Some of our early modifications of the benzophenone template centered on the central portion of the molecule, the linker region and the B-ring. A conformationally constrained version (**4**) of the

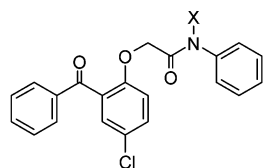
template was prepared by linking the ortho position of the C-ring to the amide of the linker region. Synthesis of this analogue, which is illustrated in Scheme 1, was accomplished by first linking the A- and B-rings, and then installing the linker region and C-ring sequentially. Metal halogen exchange of a brominated phenol derivative (**5**), followed by quenching with a Weinreb amide (**6**), allowed ready access to the A- and B-rings of the benzophenone template (**7**). Deprotection to reveal the phenol **8** then provided a handle for building the linker region via reaction with *o*-bromoethyl acetate to give **9**. Finally, the C-ring was added to the molecule via amide formation between the acid chloride **11**, derived in two steps from **9**, and a commercially available amine. The *o*-methyl analogue **12** was also prepared to allow direct comparison in the antiviral assays,⁹ and we found that the constrained analogue was less potent against both wild type and nevirapine-resistant viruses. Although the differences were not dramatic, there appeared to be some advantage to using the nonconstrained amides, such as **12**. This result is consistent with the presence of an internal hydrogen bond involving the amide NH in the enzyme-bound conformation of **12**, which is precluded in **4**.

A second modification of the linker region involved formation of the hydroxylamine derivative **13** (Figure 2). This analogue was prepared in an approach similar to that outlined in Scheme 1; an unsubstituted A-ring analogue of the acid chloride **11** was mixed with 2-phenylhydroxylamine in acetonitrile to give **13**. This structural modification, however, did not prove to be beneficial. The potency of **13** was significantly less than the corresponding des-hydroxy analogue **3**.

Finally, we explored the impact of reversing the amide in the linker region. The analogue of **3** with the amide inverted was not chemically stable, but we were able to prepare a version with the oxygen replaced by a carbon (**17**) via the route illustrated in Scheme 2. This is a different synthetic approach than the one described above. In this case, the A-ring is installed last. Acylation of the primary amine **14** with benzoyl chloride was followed by a dehydrative ring closure to give intermediate **16**. Ring opening, followed by a second reaction with benzoyl chloride, produced **17**. The results of an antiviral assay with **17** indicate the amide configuration is important, since compound **17** was far less potent against the wild-type virus than **3**.

Scheme 2. Synthesis of the Reverse Amide Linker Analogue^a

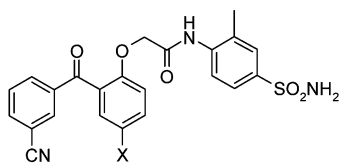
^a (a) PhCOCl, pyridine; (b) POCl₃, P₂O₅, xylene, 54%; (c) PhCOCl, triethylamine, toluene, 1 drop H₂O, 35%. IC₅₀ values determined using an acute infection assay in MT4 cells. Wild-type virus (wt) is the HIV-1 IIIB strain.



13: X = OH; IC₅₀ = 156 nM (wt), 1910 nM (nev-R)

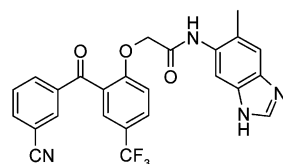
3: X = H; IC₅₀ = 22 nM (wt), 298 nM (nev-R)

Figure 2. N-Hydroxylated benzophenone analogue. The IC₅₀ values were determined using an acute infection assay in MT4 cells. Wild-type virus (wt) is the HIV-1 IIIB strain. Nevirapine resistant virus (nev-R) contains the Y181C mutation.



18a: X = CF₃; IC₅₀ = 25 nM (wt), 17 nM (nev-R)

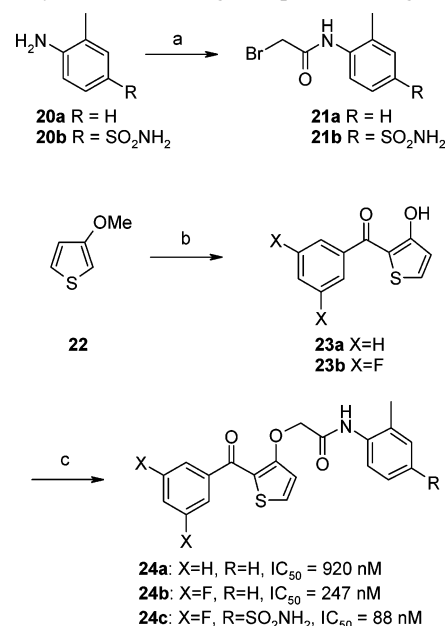
18b: X = Cl; IC₅₀ = 1 nM (wt), 2 nM (nev-R)



19 IC₅₀ = 31 nM (wt), 47 nM (nev-R)

Figure 3. Analogues with trifluoromethyl substitution on the B-ring. The IC₅₀ values were determined using an acute infection assay in MT4 cells. Wild-type virus (wt) is the HIV-1 IIIB strain. Nevirapine resistant virus (nev-R) contains the Y181C mutation.

One question we had about the B-ring in the benzophenone template was the role of the *p*-chloro substituent. Initiating the route outlined in Scheme 1 with 2-bromo-1-methoxy-4-(trifluoromethyl)benzene,¹¹ an analogue of compound **5**, allowed us to explore the impact of replacing the *p*-chloro group with a trifluoromethyl group. The two analogues shown in Figure 3 illustrate that although the trifluoro-based compounds **18a** and **19** are active against both wild type and nevirapine-resistant viral strains, they are not as potent as the corresponding chloro-substituted compound **18b**.

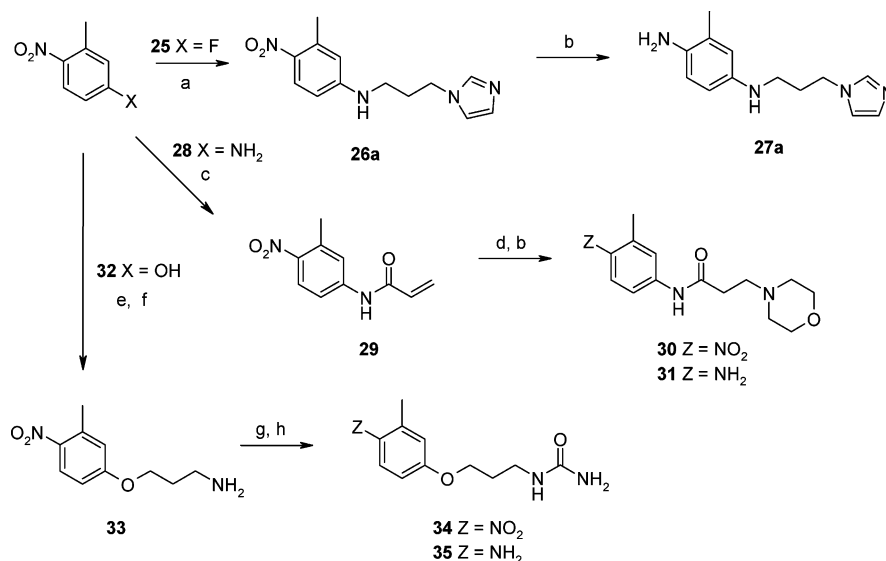
Scheme 3. Synthesis of B-Ring Thiophene Analogues^a

^a (a) BrCH₂COBr, pyr, CH₂Cl₂, 69–100%; (b) ArCOCl, AlCl₃, CH₂Cl₂, reflux, overnight, 22–40%; (c) **21**, K₂CO₃, acetone, reflux, 5–6 h, 22–77%. IC₅₀ values were determined using HIV-1 IIIB wild-type virus in an acute infection assay in MT4 cells.

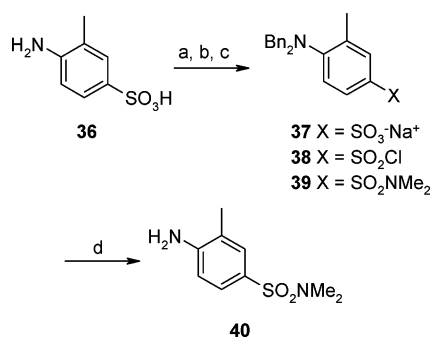
A variation of the synthetic approach of Scheme 1 allowed us to replace the aryl B-ring with a thiophene (Scheme 3). Aluminum chloride-mediated coupling of the methoxy thiophene **22** and the acid chloride derivative of the A-ring gave the A/B intermediates **23a,b**. In this case, the C-ring amide linkage was formed before installation of the A/B-rings by reaction of the arylamines **20a,b** with bromoacetyl bromide. Subsequent alkylation of **23a,b** with **21a,b** produced the desired analogues in a slightly more convergent route than the one shown above. Three versions of the thiophene B-ring analogues were prepared (**24a–c**). Again, although these compounds were active against wild-type HIV, their potency was low relative to analogues with the chlorophenyl B-ring.

SAR of the C-Ring. Since the above experimental work indicated the B-ring and linker regions of the benzophenone template were well optimized, we turned our attention to modifications of the C-ring. As noted above, previous work in this template had established the importance of an *o*-methyl group and had indicated that additional substitution at the para position could be tolerated. We chose to further explore the potential for para substitution using a synthetic approach analogous to that described in Scheme 1.

Varying the C-ring substitution required preparation of several aniline derivatives, as illustrated in Schemes 4 and 5. Scheme 4 demonstrates the flexibility of starting with various para-substituted 2-nitrotoluenes. The fluoro derivative **25** readily yielded C-rings with secondary amines at the para position (**26**) when mixed with primary amines in mild base. The para amide derivative **30** was generated from the aniline **28**. In this case, the amine of the starting material was used to form an α,β -unsaturated amide (**29**), which then gave **30** via 1,4-addition of morpholine. Ether analogues were readily obtained either by reaction of alcohols with the fluoro derivative **25** or from the phenol starting material **32**. In all cases, the desired C-ring aniline was obtained by reduction of the aryl nitro group to an amine in the final step. This routinely proceeded cleanly and in good yields.

Scheme 4. Synthesis of Aniline Intermediates for C-Ring Analogues^a

^a (a) 1-(3-aminopropyl)-imidazole, NaHCO₃, pyridine, 49%; (b) **26a** to **27a** and **30** to **31**: H₂, 10% Pd/C, MeOH, 80–100%; (c) ClC(O)CH=CH₂, Et₃N, CH₂Cl₂, 0 °C; (d) **29** to **30**: morpholine, EtOH, reflux, 80% for 2 steps (**29** to **31**); (e) 3-bromopropyl phthalimide, Cs₂CO₃, DMF, reflux; (f) H₂NNH₂·H₂O, EtOH, reflux, 85% for two steps (**32** to **33**); (g) **33** to **34**: Me₃SiN=C=O, THF, rt, 75%; (h) **34** to **35**: H₂, 10% Pd/C, EtOH, rt, 92%.

Scheme 5. Synthesis of the *p*-Sulfonamide Aniline C-Ring Intermediate^a

^a (a) **36** to **37**: BnBr, Na₂CO₃, H₂O, CH₂Cl₂, reflux; (b) **37** to **38**: thionyl chloride, DMF, 0 °C, 24% for 2 steps; (c) **38** to **39**: Me₂NH, EtOH, 0 °C, 20%; (d) H₂, 10% Pd/C, toluene, rt, 67%.

Scheme 5 exemplifies the synthesis of the *p*-sulfonamide-substituted C-rings from the sulfonic acid **36**. The protecting group strategy varies according to the desired substitution of the final product. In the case of the dimethylsulfonamide **40**, the aniline is protected with bis-benzyl groups, and the sulfonic acid is isolated as its sodium salt. Conversion to the sulfonyl chloride follows, and this intermediate reacts readily with dimethylamine to produce **39**. Deprotection of **39** then yields the aniline for the coupling reaction. The monomethyl aniline required for **42e** was prepared using the same strategy, but with an acyl protecting group.

Compounds **41a–d** were designed to explore the conversion of the ether linkage in **1** to secondary amines or amides. As illustrated in Table 1, there was little benefit to these changes relative to the unsubstituted analogue **12**. The exception is **41d**, which is potent against both the wild type and K103N mutant viruses. Replacement of the terminal amine in **1**, however, with other groups proved to be more consistently beneficial. The sulfonamide (**42a**), urea (**42b**), and ether (**42c**) substituents were all well tolerated, and these compounds were quite potent in the antiviral assays. The best results were achieved when the para position was substituted with a sulfonamide (**42d**). This analogue had excellent potency against both wild-type virus and the two key mutant viruses associated with NNRTI resistance

(K103N and Y181C). Analogues with substitution of the sulfonamide (**42e,f**) were also active in the antiviral assays, but were not quite as potent as **42d**. In general, substitution at the para position was quite well tolerated. Most of the compounds did not show dramatic differences in potency, even in cases with fairly significant changes (e.g., **42a** vs **42d**). This is consistent with the hypothesis that the para substituent reaches into a solvent pocket when bound to the HIV reverse transcriptase.

In addition to changing the substituent on the C-ring, we explored the use of pyridine rings in this position. Synthesis of the necessary anilines to form the C-rings was carried out as shown in Scheme 6. For the analogues in which the pyridine nitrogen was ortho to the sulfonamide, a chloro-substituted pyridine (e.g., **43**)¹² was converted to the corresponding thiol **44**, which could be oxidized to the desired sulfonamide **45**. Reduction of the aryl nitro group then provided the C-ring aniline **46**. Synthesis of the C-ring with the pyridine nitrogen ortho to the amine required a different approach. In this case, the pyridine **47** was sulfonlated to give an intermediate sulfonic acid, the aniline group of which was protected to give **48**. The sulfonic acid was then converted to the desired sulfonamide **49** in a single step.

The synthesis of the A/B-rings of the C-ring pyridine analogues is a variation on the Scheme 1 approach (Scheme 7). In this case, the Weinreb amide derivative was made of the B-ring (**52**) for reaction with the lithiated A-ring. The A-rings were derived from bromo aryl derivatives. The bromo groups provided the access point for all three of the A-ring substituents. We started with 1,3,5-tribromobenzene (**50**) and carried out a pair of metal–halogen exchange reactions, quenching the first with hexachloroethane and the second with Weinreb amide **52**, to give **53a**. The final bromo group acted as a cyano surrogate, and it was converted using a palladium-mediated reaction with sodium cyanide to provide **54a**, which was readily deprotected to **55a** and then converted to the analogues shown in Table 2.

In addition to the C-ring sulfonamide intermediates prepared in Scheme 6, two commercially available pyridine-rings were used to prepare **56a,b**. These analogues provided further confirmation of the above observations that the *p*-sulfonamide group is quite beneficial (Table 2). In the series of sulfonamide

Table 1. SAR of Para Substituents on the C-Ring^a

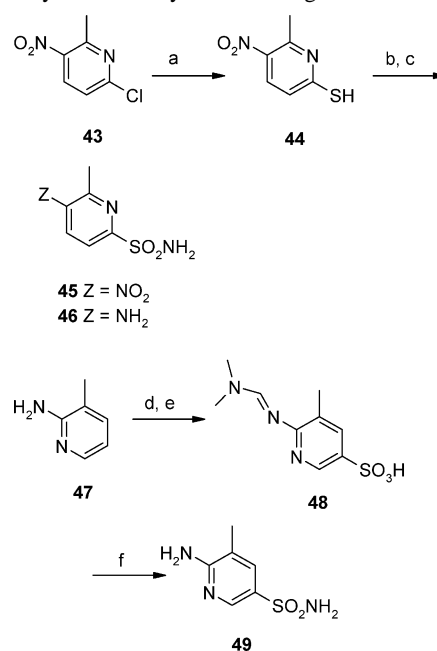
	X	R	Potency (IC ₅₀ , nM)			
			wt ^b	wt ^c	K103N ^c	Y181C ^c
12	F	H	25	8	38	25
41a	F		37	na	158	na
41b	F		18	na	109	na
41c	F		41	na	96	na
41d	F		5	na	9	na
42a	CF ₃		7	3	4	6
42b	CF ₃		6	4	4	10
42c	CF ₃		6	6	16	12
42d	CF ₃	SO ₂ NH ₂	1	2	2	3
42e	CF ₃	SO ₂ NHMe	8	3	2	na
42f	CF ₃	SO ₂ NMe ₂	10	8	6	na

^a Synthesis: **41a**, **41b**, **41c**, and **42c** prepared from **25**; **41d** prepared from **28**; **42b** prepared from **32**; **42e** and **42f** prepared from **36**. ^b IC₅₀ values were determined using HIV-1 III B wild-type virus in an acute infection assay in MT4 cells. ^c IC₅₀ values were determined using a HeLa MAGI assay system. The wild-type virus was the HxB2 strain, and the K103N and Y181C mutants were isogenic with the HxB2 virus backbone.

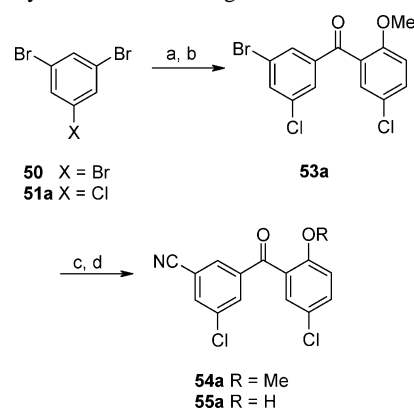
derivatives (**57–59**), placement of the pyridine nitrogen at the X₃ position (**59**) attenuated potency against both wild type and K103N mutant viruses. Placement of the pyridine nitrogen at either the X₁ (**57a,b**) or X₂ (**58a,b**) positions, however, gave analogues with excellent potency against both wild type and mutant viruses.

SAR of the A-Ring. After establishing the flexibility of C-ring substitution, we turned to the A-ring for further optimization work. In this case, relatively small changes in structure did prove to have a significant impact on the potency of the analogues.

Our first step was to explore the impact of moving a small substituent around the A-ring. In this case, the A/B-rings were prepared as illustrated in Scheme 8. The A-ring source was a substituted benzoyl chloride (e.g., **60a**), which readily underwent Friedel–Crafts acylation with 4-chloroanisole to produce the A/B-ring structure **61a**. The aluminum salts which catalyzed the Friedel–Crafts reaction also removed the methoxy group, conveniently exposing the phenol for the subsequent alkylation step. The C-ring for this analogue set was prepared in a fashion analogous to that shown in Scheme 4. The *p*-fluoro group of the nitrotoluene **25** was displaced with thiomorpholine. Subsequent oxidation of the thioether to a sulfoxide and reduction of the aryl

Scheme 6. Synthesis of Pyridine C-Ring Intermediates^a

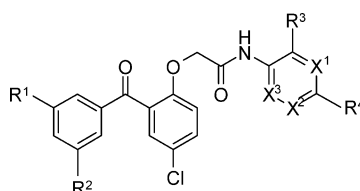
^a (a) thiourea, EtOH and then KOH, 30%; (b) **44** to **45**: 1N HCl, Cl₂ and then NH₃/CH₂Cl₂, 40%; (c) **45** to **46**: H₂, 10% Pd/C, EtOH; (d) H₂SO₄/SO₃, 160 °C, 50%; (e) SOCl₂, DMF, rt, 77%; (f) PCl₅ and then NH₄OH, rt, 45%.

Scheme 7. Synthesis of A/B-Ring Intermediates^a

^a (a) **50** to **51a**: *n*-BuLi, Et₂O, -78 °C; then, Cl₃CCl₃, -78 °C to room temperature, 92%; (b) **51a** to **53a**: *n*-BuLi, Et₂O, -78 °C; then, 5-chloro-N,2-dimethoxy-N-methyl benzamide (**52**), -78 °C to room temperature, 97%; (c) **53a** to **54a**: CuI, NaCN, Pd(PPh₃)₄, MeCN, reflux, 56%; (d) **54a** to **55a**: BBr₃, CH₂Cl₂, -78 °C to room temperature, 100%.

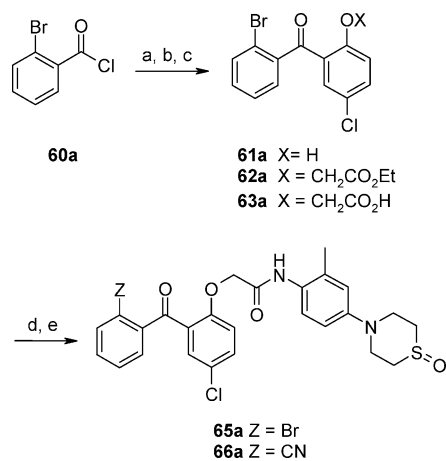
nitro group produced the desired aniline **64**. In this case, the A/B-ring was not converted to an acid chloride. Instead, HOBT-mediated coupling was used to partner the acid **63a** with the aniline **64** to give **65a**. As was the case in Scheme 7, the bromo substituent on the A-ring was converted to cyano group in the final step. In the case of the *m*-cyano analogue **66b**, the cyano-substituted acid chloride A-ring starting material was commercially available and the cyano group was carried through the synthesis.

In Table 3, we show representative results of the impact of moving the A-ring substituent. Clearly, placement of a small group at the meta position (**66b**) is far more favorable than substitution of the same group at the ortho (**66a**) or para (**66b**) position. Furthermore, substitution at the meta position offers an advantage over the unsubstituted analogue **67**, particularly against the critical mutant viruses, K103N and Y181C. In fact, subsequent crystallography demonstrated that tyrosine residues 181 and 188 tolerated meta substitution.⁸

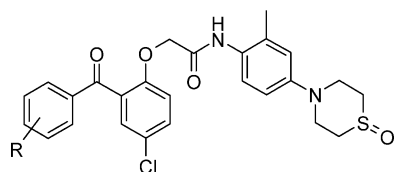
Table 2. SAR of C-Ring Pyridyl Analogues

compound	R ¹	R ²	R ³	R ⁴	X ¹	X ²	X ³	potency (IC ₅₀ , nM) ^a			
								wt	K103N	Y181C	V106A
56a	F	F	H	Cl	CH	N	CH	--	67	--	--
56b	F	F	H	OMe	CH	N	CH	--	72	--	--
57a	Me	CN	Me	SO ₂ NH ₂	N	CH	CH	2	6	4	3
57b	Cl	CN	Me	SO ₂ NH ₂	N	CH	CH	1	3	3	7
58a	Me	CN	Me	SO ₂ NH ₂	CH	N	CH	1	7	4	2
58b	Cl	CN	Me	SO ₂ NH ₂	CH	N	CH	2	5	2	10
59	Me	CN	Me	SO ₂ NH ₂	CH	CH	N	18	93	--	--

^a IC₅₀ values were determined using a HeLa MAGI assay. Wild-type virus (wt) was the HxB2 strain. K103N, Y181C, and V106A mutants were isogenic with the HxB2 virus backbone.

Scheme 8. Synthesis of A-Ring Monosubstituted Analogues^a

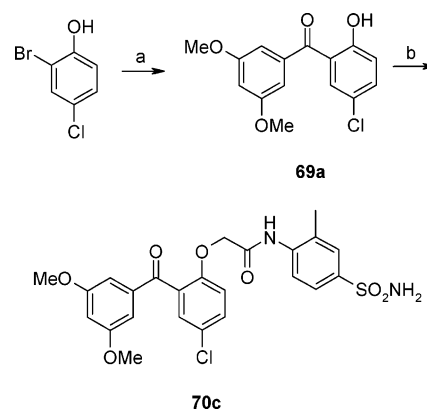
^a (a) **60a** to **61a**: AlCl₃, 4-chloroanisole, CH₂Cl₂, reflux, 96%; (b) **61a** to **62a**: Br₂CH₂CO₂Et, K₂CO₃, acetone, reflux; (c) **62a** to **63a**: LiOH, H₂O, EtOH, THF, rt, 98% for two steps; (d) HOBT, EDAC-HCl, 2-methyl-4-(1-oxido-4-thiomorpholinyl)aniline (**64**), Et₃N, 22%; (e) CuCN, DMF, 16 °C, 11%.

Table 3. SAR of Monosubstituted A-Ring Analogues

R	potency (IC ₅₀ , nM) ^a				
	wt	K103N	Y181C	V106A	
67	H	17	100	150	1400
66a	<i>o</i> -CN	1500	155	700	2000
66b	<i>m</i> -CN	4	5	6	na
66c	<i>p</i> -CN	26	44	355	1400

^a IC₅₀ values determined using a HeLa-MAGI assay. Wild-type virus (wt) was the HxB2 strain. K103N, Y181 C, and V106A mutants were isogenic with the HxB2 virus backbone.

Our further exploration of meta substitution patterns in the A-ring began to focus on disubstitution. A number of examples were prepared using two different approaches for building the A/B-ring. Method A, a variation of the approach shown in Scheme 1, is shown in Scheme 9. As in Scheme 1, the A-ring was formed from a Weinreb amide, readily accessed from the

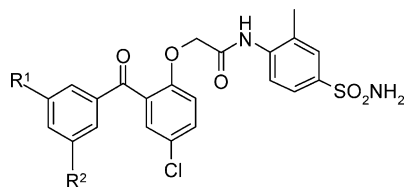
Scheme 9. Synthesis of Disubstituted A/B-Ring Intermediates^a

^a (a) 2.2 equiv *n*-BuLi, THF, -78 °C; then, *N*-methyl-*N*,3,5-tris(methoxy)benzamide (**68**), -78 °C to room temperature, 20%; (b) **21b**, K₂CO₃, acetone, reflux, 66%.

commercially available benzoyl chloride derivatives. The difference from Scheme 1 is the B-ring origin. In this case, 2-bromo-4-chlorophenol, rather than the anisole derivative, provided the B-ring. When two equivalents of *n*-BuLi were used in THF instead of ether, a dianion was formed by deprotonation and metal-halogen exchange. Reaction with the Weinreb amide then provided the A/B-ring, which did not require a deprotection step before the alkylation to attach the linker region and C-ring. Method B is the approach described in Scheme 7. The B-ring source was the Weinreb amide **52**, and the A-rings were formed from metal halogen exchange of di-*meta*-substituted aryl bromides. Since the C-ring was not varied in this analogue set, it was most efficient to attach the linker to the C-ring before alkylation of the B-rings. This is similar to the approach shown in Scheme 3, using **21b**. More efficient alkylations were achieved with the addition of two equivalents of sodium iodide to the reaction mixture.

Chan et al. have previously disclosed the mono-*meta* substituted analogue **18b**,⁷ which is a very potent compound, but does show some diminution of potency against a V106A mutant virus (Table 4). Addition of a methyl group (**70g**) or a chloro group (**70h**) at the second *meta* position on the A-ring had a dramatic impact on the ability of the analogue to inhibit the V106A strain, without sacrificing the potency in the wild type, K103N, and Y181C viruses.

We made a number of analogues to explore the impact of di-*meta* substitution, particularly on the mutant viruses. Most

Table 4. SAR of Disubstituted A-Ring Analogues

method ^b	R ¹	R ²	potency (IC ₅₀ , nM) ^a			
			wt	K103N	Y181C	V106A
18b	H	CN	0.7	1.5	1.5	30
42d	F	CF ₃	1.4	2.0	2.9	10.5
70a	A	OMe	16	370	13	500
70b	A	Me	0.4	3.3	3.0	4.2
70c	B	Br	30	93	290	18
70d	B	Cl	2.2	6.1	6.9	13
70e	B	Cl	1.2	3.6	3.3	9.4
70f	A	(N)	16	140	450	18
70g	B	Me	0.5	0.9	1.9	1.4
70h	B	Cl	0.5	1.0	0.7	3.4
70i	B	CF ₃	1.0	1.1	2.0	5.6
EFV ^c			0.8	25	1.6	1.8
NVP ^c			88	5800	10300	8200

^a IC₅₀ values determined using a HeLa MAGI assay. Wild-type virus (wt) was the HxB2 strain. K103N, Y181 C, and V106A mutants were isogenic with the HxB2 virus backbone. ^b Method A is shown in Scheme 9; method B is shown in Scheme 7. ^c EFV is efavirenz; NVP is nevirapine.

of these analogues had very good profiles against the wt, K103N, Y181C, and V106A viruses, including the fluoro, trifluoromethyl (**42d**), the chloro, bromo (**70d**), and the chloro, methyl (**70e**). Although all of these were more potent against the V106A strain than the mono-meta substituted analogue, they were not quite as potent as the methyl, cyano analogue **70g**. There appear to be some size restrictions to the di-meta substitution approach. For example, the bromo, trifluoromethyl analogue **70c** is significantly less potent across the panel than its fluoro, trifluoromethyl counterpart **42d**.

Use of electron-donating substituents (**70a**) was clearly less favorable than electron withdrawing substituents, although potency against the Y181C mutant virus was less affected than potency against the other viruses in the panel. Use of neutral substituents (methyl groups), however, was very well tolerated. In fact, the dimethyl analogue **70b** was similar in potency to the methyl, cyano analogue **70g**.

In addition to di-meta substitution, we also explored replacement of the meta-substituted phenyl ring with a meta-substituted pyridine (**70f**). In this case, although the wild type and V106A mutants were still fairly sensitive, the K103N and Y181C mutants were not.

In summary, we have developed several variants of benzophenone syntheses and used them to systematically explore the A-ring, B-ring, linker region, and C-ring sections of this novel template. Our efforts have culminated in the discovery of very potent analogues, including **70g** and **70h**, both of which compare quite favorably to efavirenz and nevirapine in vitro and offer potential advantages in the treatment of virus resistant to the current NNRTIs.

Selection of 70h (GW678248). Table 4 illustrates a situation that is not unusual in drug discovery: we have identified more than one compound with an attractive potency profile in our primary assays. Multiple analogues had excellent antiviral activity against both wild type and mutant viruses, particularly those associated with clinical resistance to efavirenz and nevirapine. The selection of a good drug candidate, however, does not depend on in vitro potency alone, and we obtained some preliminary pharmacokinetic data to help distinguish between the most potent benzophenones.

Intravenous plasma concentration vs time plots of two of the most potent compounds are shown in Figure 4. In all three of the species studied, **70h** had a lower clearance rate and longer elimination half-life than **70g**. This is consistent with our hypothesis that metabolism of the aryl methyl group in **70g** was blocked when that methyl was replaced by the chloro group in **70h**. On the basis of the potency in antiviral assays and the initial pharmacokinetics data, **70h** was selected for further preclinical evaluation and development.

Conclusions

The benzophenone template for NNRTI inhibitors has been transformed from a lead with moderate activity against wild type HIV and little or no activity against clinically relevant mutants to a very promising series with excellent in vitro potency against both wild type and key mutant viruses, including the Y181C mutation associated with nevirapine resistance and the K103N mutation associated with efavirenz resistance. In particular, **70h** (GW678248) has very low IC₅₀ values in antiviral assays: 0.5 nM against wild-type virus, 1 nM against K103N, and 0.7 nM against Y181C. Compound **70h** has also demonstrated relatively low clearance in intravenous pharmacokinetic studies in three species. On the basis of this very promising profile, GW678248 was selected for further development. It has been converted to a prodrug to increase its oral bioavailability, which progressed to phase 2 clinical trials.

Experimental Section

NMR spectra were recorded on a Varian XL200, Varian Unity Plus 400, or Varian Unity Plus 200 MHz spectrometers. Elemental analyses were carried out by Atlantic Microlabs, Inc., Atlanta, GA.

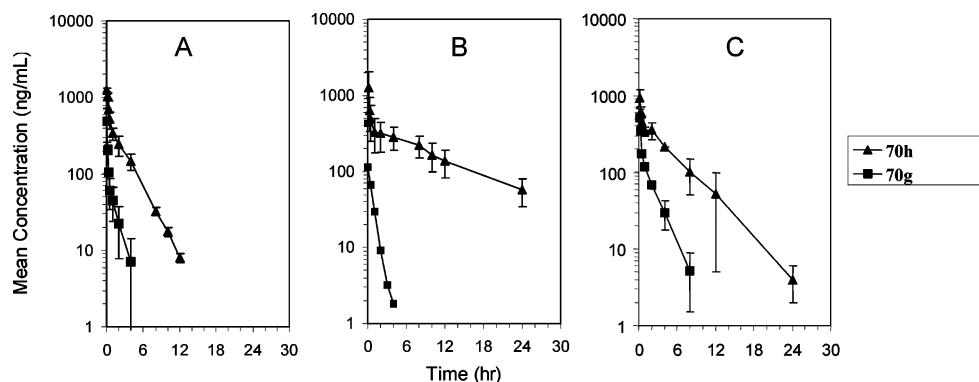


Figure 4. Plasma concentration–time profiles of **70g** and **70h** (GW678248) in rats (A), dogs (B), and cynomolgus monkeys (C) following intravenous administration at 1 mg/kg.

Some mass spectral data were obtained using atmospheric pressure chemical ionization (APCI). All purchased starting materials were used without further purification. All solvents were reagent grades. Unless otherwise noted, all reactions were run in oven-dried, round-bottomed flasks under nitrogen atmosphere. Representative procedures are included below for compounds **4**, **6**, **7–13**, **15–17**, **21b**, **23b**, **24c**, **26a**, **27a**, **29–31**, **33–35**, **37–40**, **44–46**, **48**, **49**, **51a**, **52**, **53a**, **54a**, **55a**, **61a**, **63a**, **65a**, **66a**, **69a**, and **70h**. The syntheses of reference compounds **3**,⁶ **18b**,⁷ **42a**,⁷ and **42d**⁷ have been previously published. Procedures and characterization data for all other intermediates and final products can be found in the Supporting Information.

3,5-Difluoro-*N*-methoxy-*N*-methylbenzamide (6): Triethylamine (20 mL) was added to a solution of *N,O*-dimethylhydroxylamine hydrochloride (4.74 g, 48.6 mmol) in CHCl_3 (100 mL), and the mixture was cooled to 0 °C. 3,5-Difluorobenzoyl chloride (6.60 g, 37.4 mmol) was added dropwise over 5 min. The reaction was stirred at 0 °C for 35 min and then allowed to warm to room temperature over 1 h. The reaction mixture was partitioned between EtOAc (200 mL) and water (100 mL). The organic layer was washed with water (100 mL) and brine, dried over MgSO_4 , filtered, and concentrated in vacuo to give **6** (6.963 g, 93%): $^1\text{H NMR}$ (400 MHz, CDCl_3) δ 7.27–7.22 (m, 2H), 6.94–6.89 (m, 1H), 3.57 (s, 3H), 3.37 (s, 3H) ppm.

(5-Chloro-2-methoxyphenyl)(3,5-difluorophenyl)methanone (7): *n*-BuLi (11.3 mL of 1.6 M solution in hexanes, 18.2 mmol) was added dropwise over 4 min to a solution of 2-bromo-4-chloroanisole (2.2 mL, 15.8 mmol) in Et_2O (100 mL) cooled to –78 °C. The resulting mixture was stirred at –78 °C for 20 min, and then a solution of **6** (3.49 g, 17.3 mmol) in Et_2O (5 mL) was added dropwise over 5 min. The reaction mixture was stirred at –78 °C for 1 h and then allowed to warm to room temperature over 3.25 h. The reaction was quenched by adding water (20 mL) and stirring for 20 min. The mixture was then partitioned between water (100 mL) and Et_2O (100 mL). The aqueous layer was extracted with Et_2O (50 mL), and the combined organic layers were dried over MgSO_4 , filtered, and concentrated in vacuo to give 5.191 g of crude material. Purification by flash chromatography using 3% EtOAc/hexanes as eluant gave **7** (1.861 g, 42%) as a white solid: $^1\text{H NMR}$ (400 MHz, CDCl_3) δ 7.44 (dd, $J = 2.5$, 8.9 Hz, 1H), 7.32 (d, $J = 2.9$ Hz, 1H), 7.29–7.24 (m, 2H), 7.03–6.97 (m, 1H), 6.92 (d, $J = 8.9$ Hz, 1H), 3.70 (s, 3H) ppm; $^{13}\text{C NMR}$ (100 MHz, CDCl_3) δ 192.6, 163.0 ($J_{\text{CF}} = 11.5$, 250 Hz), 156.1, 140.6, 132.5, 129.5, 129.0, 126.2, 113.1, 112.6 ($J_{\text{CF}} = 6.9$, 19.1 Hz), 108.6 ($J_{\text{CF}} = 25.6$ Hz), 56.2 ppm.

(5-Chloro-2-hydroxyphenyl)(3,5-difluorophenyl)methanone (8): BBr_3 (9.8 mL of 1.0 M solution in CH_2Cl_2 , 9.80 mmol) was added dropwise over 20 min to a solution of **7** (1.847 g, 6.53 mmol) in CH_2Cl_2 (65 mL) at –78 °C. The resulting mixture was stirred at –78 °C for 35 min and then allowed to warm to room temperature over 1.5 h. The reaction mixture was poured onto ice, stirred for 30 min, and extracted with CH_2Cl_2 (50 mL). The organic layer was washed with brine, dried over MgSO_4 , filtered, and concentrated in vacuo to give **8** (1.725 g, 98%): MS (ES–) m/z 267 (M – H); $^1\text{H NMR}$ (400 MHz, CDCl_3) δ 11.58 (s, 1H), 7.49–7.47 (m, 2H), 7.19–7.1 (m, 2H), 7.06–7.03 (m, 2H) ppm.

Ethyl [4-chloro-2-(3,5-difluorobenzoyl)phenoxy]acetate (9): A mixture of **8** (1.72 g, 6.40 mmol), K_2CO_3 (3.98 g, 28.8 mmol), and ethyl bromoacetate (0.82 mL, 7.36 mmol) in acetone (45 mL) was heated to reflux for 4.33 h. The reaction mixture was then partitioned between EtOAc (130 mL) and water (100 mL). The aqueous layer was extracted with EtOAc (30 mL). The combined organic layers were then dried over MgSO_4 , filtered, and concentrated in vacuo to give **9** (2.321 g, 100%): $^1\text{H NMR}$ (400 MHz, $\text{DMSO}-d_6$) δ 7.43–7.34 (m, 4H), 7.02–6.99 (m, 1H), 6.77 (d, $J = 8.5$ Hz, 1H), 4.52 (s, 2H), 4.18 (q, $J = 7.1$ Hz, 2H), 1.22 (t, $J = 7.1$ Hz, 3H) ppm.

[4-Chloro-2-(3,5-difluorobenzoyl)phenoxy]acetic acid (10): A suspension of **9** (6.40 mmol), $\text{LiOH}\cdot\text{H}_2\text{O}$ (0.671 g, 16.0 mmol), EtOH (5 mL), water (5 mL), and THF (20 mL) was stirred at room temperature for 2.75 h. The pH was adjusted to 5 using 1 N HCl

(aq), and the mixture was then partitioned between EtOAc (50 mL) and water (50 mL). The aqueous layer was extracted with EtOAc (35 mL), and the combined organic layers were dried over MgSO_4 , filtered, and concentrated in vacuo to give **10** (1.691 g, 81%): MS (ES–) m/z 325 (M – H); $^1\text{H NMR}$ (400 MHz, $\text{DMSO}-d_6$) δ 7.54–7.50 (m, 3H), 7.48 (dd, $J = 2.7$, 9.1 Hz, 1H), 7.36 (d, $J = 2.7$ Hz, 1H), 6.93 (d, $J = 9.1$ Hz, 1H), 4.27 (s, 2H) ppm; $^{13}\text{C NMR}$ (100 MHz, $\text{DMSO}-d_6$) δ 192.9, 162.9 ($J_{\text{CF}} = 12$, 248 Hz), 155.7, 140.4 ($J_{\text{CF}} = 8$ Hz), 132.4, 129.1, 129.0, 124.6, 115.7, 113.3 ($J_{\text{CF}} = 26$ Hz), 109.5 ($J_{\text{CF}} = 26$ Hz), 67.6 ppm.

[4-Chloro-2-(3,5-difluorobenzoyl)phenoxy]acetyl chloride (11): Oxalyl chloride (2.7 mL of 2.0 M solution in CH_2Cl_2 , 5.44 mmol) was added dropwise over 14 min to a solution of **10** (0.611 g, 2.04 mmol) in DMF (0.10 mL) and CH_2Cl_2 (12 mL). The resulting mixture was stirred at room temperature for 2.25 h then concentrated in vacuo. The crude product was used immediately without further purification or characterization.

{5-Chloro-2-[2-(2,3-dihydro-1*H*-indol-1-yl)-2-oxoethoxy]phenyl}(3,5-difluorophenyl)methanone (4): A solution of **11** (0.51 mmol) in acetone (2 mL) was added dropwise over 2 min to a mixture of indoline (0.05 mL, 0.44 mmol), acetone (5 mL), sodium bicarbonate (0.384 g, 8.97 mmol), and water (0.5 mL), and the resulting mixture was stirred at room temperature for 2.5 h. The mixture was then poured into EtOAc (50 mL) and water (25 mL). The aqueous layer was separated and extracted with EtOAc (25 mL). The combined organic layers were dried over MgSO_4 , filtered in concentrated in vacuo to yield 0.278 g of a yellow oil. Purification by flash chromatography using 25% EtOAc/hexanes as eluant, followed by crystallization from CH_2Cl_2 /hexanes gave **4** (0.069 g, 37%) as white crystals: mp 158–160 °C; $^1\text{H NMR}$ (400 MHz, CDCl_3) δ 8.14 (d, $J = 8.2$ Hz, 1H), 7.44–7.39 (m, 4H), 7.22–7.18 (m, 2H), 7.07–6.97 (m, 3H), 4.70 (s, 2H), 3.98 (t, $J = 8.2$ Hz, 2H), 3.18 (t, $J = 8.2$ Hz, 2H) ppm; $^{13}\text{C NMR}$ (100 MHz, CDCl_3) δ 190.1, 162.5, 160.8 ($J_{\text{CF}} = 251.7$ Hz), 152.4, 140.4, 138.1, 130.3, 128.9, 127.4, 127.3, 125.7, 125.0, 122.7, 122.6, 115.2, 112.6, 110.7 ($J_{\text{CF}} = 26.7$ Hz), 106.7 ($J_{\text{CF}} = 25.1$ Hz), 66.8, 44.9, 26.4 ppm; IR (KBr) 1676, 1657 cm^{-1} ; MS (ES+) m/z 428 (M + H); Anal. ($\text{C}_{23}\text{H}_{16}\text{NO}_3\text{ClF}_2 + 0.28$ equiv H_2O) C, H, N.

2-[4-Chloro-2-(3,5-difluorobenzoyl)phenoxy]-*N*-(2-methylphenyl)acetamide (12): Prepared in a method analogous to that described for **4** above from acid chloride **11** (0.50 mmol) and *o*-toluidine (0.05 mL, 0.43 mmol). Purification by flash chromatography using 10% EtOAc/hexanes as eluant gave **12** (0.121 g, 58%) as a white solid: $^1\text{H NMR}$ (400 MHz, CDCl_3) δ 8.30 (br s, 1H); 7.71 (d, $J = 8.6$ Hz, 1H), 7.53 (dd, $J = 2.5$, 8.6 Hz, 1H), 7.36 (d, $J = 2.5$ Hz, 1H), 7.34–7.31 (m, 2H), 7.22–7.17 (m, 2H), 7.09 (app t, $J = 7.1$ Hz, 1H), 7.05–7.01 (m, 2H), 4.77 (s, 2H), 2.18 (s, 3H) ppm; $^{13}\text{C NMR}$ (100 MHz, CDCl_3) δ 191.6, 165.4, 163.1 ($J_{\text{CF}} = 12$, 252 Hz), 154.3, 139.9 ($J_{\text{CF}} = 7.6$ Hz), 134.7, 133.4, 130.8, 130.5, 130.3, 128.1, 127.3, 126.8, 126.0, 123.7, 114.8, 113.1 ($J_{\text{CF}} = 7.6$, 19 Hz), 109.4 ($J_{\text{CF}} = 26$ Hz), 68.1, 17.7 ppm; MS (ES+) m/z 416 (M + H), 438 (M + Na); Anal. ($\text{C}_{22}\text{H}_{16}\text{NO}_3\text{ClF}_2$) C, H, N.

2-(2-Benzoyl-4-chlorophenoxy)-*N*-hydroxy-*N*-phenylacetamide (13): 2-(2-Benzoyl-4-chlorophenoxy)acetyl chloride⁶ (0.1 g, 32 mmol) was dissolved in dry MeCN (2 mL), and a solution of 2-phenylhydroxylamine¹³ (0.35 g, 32 mmol) in MeCN (2 mL) was added. The resulting mixture was stirred at room temperature for 3 h and then filtered and concentrated in vacuo. Silica gel chromatography (elution with 25% EtOAc/hexanes) gave **13** (0.062 g, 50%): MS (APCI+) m/z 404 (M + Na); $^1\text{H NMR}$ (400 MHz, CDCl_3) δ 9.85 (s, 1 H), 7.85–7.0 (m, 13 H), 4.95 (s, 2H) ppm; HRMS (ES+) m/z Calcd. 382.08406; Exp. 382.08409 (M + H).

***N*-[2-(4-Chlorophenyl)ethyl]benzamide (15)**: Benzoyl chloride (3.9 mL, 33.7 mmol) was added in one portion to a solution of 2-(4-chlorophenyl)ethanamine (**14**) (5 g, 32.1 mmol) in pyridine (50 mL) at 0 °C. The reaction mixture was then allowed to warm to room temperature over 1.67 h and then poured into 200 mL of water/ice mixture. Product **15** was then collected by filtration, washed with four portions of water, and dried in vacuo. $^1\text{H NMR}$ (400 MHz, CDCl_3) δ 7.68–7.66 (m, 2H), 7.47 (d, $J = 7.2$ Hz,

1H), 7.38–7.42 (m, 2H), 7.28 (d, $J = 8.2$ Hz, 2H), 7.16 (d, $J = 8.2$ Hz, 2H), 6.09 (br s, 1H), 3.71–3.65 (m, 2H), 2.90 (t, $J = 6.8$ Hz, 2H) ppm; ^{13}C NMR (100 MHz, CDCl_3) δ 168.6, 138.5, 135.6, 133.4, 132.6, 131.2, 129.9, 129.7, 127.9, 42.2, 36.2 ppm.

7-Chloro-1-phenyl-3,4-dihydroisoquinoline (16): Solution of **15** (1.18 g, 4.5 mmol) in *p*-xylene (25 mL) warmed to reflux to remove water and then removed from heat. POCl_3 (10 g) and P_2O_5 (5 g) were added, and the mixture was heated at reflux for 6 h. The xylene was decanted, and the solid residue was dissolved in water. The aqueous layer was extracted with three portions of ether. The combined organic layers were then concentrated in vacuo. Silica gel chromatography (elution with 20–33% EtOAc/hexanes) gave **16** (0.5 g, 54%): MS (AP+) m/z 242 (M + H); ^1H NMR (300 MHz, CDCl_3) δ 7.60–7.57 (m, 2H), 7.48–7.43 (m, 3H), 7.37 (dd, $J = 2.1, 8.0$ Hz, 1H), 7.26–7.21 (m, 2H), 3.88–3.83 (m, 2H), 2.80–2.75 (m, 2H) ppm.

N-[2-(2-Benzoyl-4-chlorophenyl)ethyl]benzamide (17): A mixture of **16** (0.1 g, 0.41 mmol), benzoyl chloride (0.2 mL, 1.7 mmol), and triethylamine (0.1 mL, 0.72 mmol) in toluene (1 mL) and a few drops of water was stirred at room temperature for 2 h. The reaction mixture was washed with brine, dried over MgSO_4 , filtered, and concentrated in vacuo. Silica gel chromatography (elution with 20–50% EtOAc/hexanes) gave **17** (0.053 g, 35%): ^1H NMR (300 MHz, CDCl_3) δ 7.95–7.92 (m, 2H), 7.86–7.69 (m, 4H), 7.57 (d, $J = 2.1$ Hz, 1H), 7.50 (d, $J = 8.2$ Hz, 1H), 7.32–7.29 (m, 5H), 4.22–4.17 (m, 2H), 3.24–3.19 (m, 2H) ppm; ^{13}C NMR (100 MHz, CDCl_3) δ 195.8, 165.6, 137.8, 135.5, 132.4, 132.2, 130.4, 129.9, 129.3, 129.2, 128.7, 126.8, 126.7, 126.5, 125.1, 40.1, 29.3 ppm; Anal. ($\text{C}_{22}\text{H}_{18}\text{NO}_2\text{Cl} + 0.2$ equiv H_2O) C, H, N.

N-[4-(Aminosulfonyl)-2-methylphenyl]-2-bromoacetamide (21b): A solution of 4-amino-3-methylbenzenesulfonamide (**20b**)⁷ (5.0 g, 26.85 mmol) and pyridine (2.4 mL, 29.53 mmol) in CHCl_3 (150 mL) was cooled to 0 °C in an ice bath. Bromoacetyl bromide (2.6 mL, 29.53 mmol) was added dropwise over 20 min, and the resulting mixture was allowed to warm to room temperature overnight. The reaction mixture was then poured into water (150 mL) and extracted with two 100-mL portions of CH_2Cl_2 . The aqueous layer was then filtered to give crude product as a beige solid. The crude material was suspended in 1 N HCl and then filtered and washed with CH_2Cl_2 , MeOH, and hexane to give **21b** (5.705 g, 69%): ^1H NMR (400 MHz, $\text{DMSO}-d_6$) δ 9.84 (s, 1H), 7.66–7.56 (m, 3H), 7.23 (br s, 2H), 4.09 (s, 2H), 2.24 (s, 3H) ppm; ^{13}C NMR (100 MHz, $\text{DMSO}-d_6$) δ 166.0, 141.2, 139.4, 132.3, 128.4, 124.9, 124.4, 30.5, 18.4 ppm; Anal. ($\text{C}_9\text{H}_{11}\text{N}_2\text{O}_3\text{BrS}$) C, H, N.

(3,5-Difluorophenyl)(3-hydroxy-2-thienyl)methanone (23b): A mixture of 3-methoxythiophene (**22**) (1.14 g, 10 mmol), AlCl_3 (2.70 g, 20.2 mmol), and 3,5-difluorobenzoyl chloride (1.18 mL, 10 mmol) in CH_2Cl_2 (50 mL) was heated to reflux for 20 h and then stirred an additional 27 h at room temperature. The reaction mixture was then poured over ice and stirred for 40 min, and the aqueous layer was separated and extracted with CH_2Cl_2 (20 mL). The combined organic layers were dried over MgSO_4 , filtered, and concentrated in vacuo to give a dark brown solid (1.214 g). Purification by flash chromatography using 2% EtOAc/hexanes gave **23b** (0.518 g, 22%) as a yellow solid: ^1H NMR (400 MHz, CDCl_3) δ 12.04 (s, 1H), 7.57 (d, $J = 5.5$ Hz, 1H), 7.43 (dd, $J = 2.1, 7.3$ Hz, 2H), 7.02–6.97 (m, 1H), 6.84 (d, $J = 5.5$ Hz, 1H) ppm; ^{13}C NMR (100 MHz, CDCl_3) δ 188.2, 169.7, 163.1 ($J_{\text{CF}} = 12.2, 252$ Hz), 141.2, 135.9, 120.2, 111.9, 111.6 ($J_{\text{CF}} = 7.6, 19.1$ Hz), 107.9 ($J_{\text{CF}} = 25.2$ Hz) ppm.

N-[4-(Aminosulfonyl)-2-methylphenyl]-2-[[2-(3,5-difluorobenzoyl)-3-thienyl]oxy]acetamide (24c): A mixture of **23b** (0.192 g, 0.80 mmol), **21b** (0.252 g, 0.82 mmol), and K_2CO_3 (0.498 g, 3.6 mmol) in acetone (10 mL) was warmed to reflux for 6 h. The reaction mixture was then poured into water (30 mL) and extracted with two 30-mL portions of EtOAc. The combined organic layers were dried over MgSO_4 , filtered, and concentrated in vacuo to give 0.272 g of crude material. Purification by flash chromatography using 35–50% EtOAc/hexanes as eluent gave **24c** as a yellow solid (0.103 g, 28%): ^1H NMR (400 MHz, CDCl_3) δ 9.47 (br s, 1H),

8.06 (d, $J = 5.6$ Hz, 1H), 7.72–7.52 (m, 3H), 7.50–7.40 (m, 3H), 7.26 (br s, 2H), 7.17 (d, $J = 5.6$ Hz, 1H), 4.89 (s, 2H), 2.23 (s, 3H) ppm; ^{13}C NMR (100 MHz, CDCl_3) δ 185.0, 166.7, 166.6, 162.5 ($J_{\text{CF}} = 13, 248$ Hz), 160.1, 142.5, 139.1 ($J_{\text{CF}} = 12$ Hz), 136.3, 132.0, 131.8, 128.4, 124.5, 124.4, 120.0, 119.0, 112.5 ($J_{\text{CF}} = 27$ Hz), 107.8 ($J_{\text{CF}} = 26$ Hz), 18.3, 14.4 ppm; MS (ES+) m/z 467 (M + H), 489 (M + Na); Anal. ($\text{C}_{26}\text{H}_{16}\text{N}_2\text{O}_5\text{F}_2\text{S}_2$) C, H, N.

N-[3-(1H-Imidazol-1-yl)propyl]-3-methyl-4-nitroaniline (26a): A mixture of 5-fluoro-2-nitrotoluene (0.24 mL, 2.0 mmol), 1-(3-aminopropyl)-imidazole (0.41 mL, 3.4 mmol), and sodium bicarbonate (0.302 g, 3.6 mmol) in pyridine (5 mL) and water (0.5 mL) was heated to reflux for 3 h. The reaction mixture was then partitioned between water (50 mL) and EtOAc (50 mL). The organic layer was concentrated to give a yellow solid, which was purified by crystallization from EtOAc/hexanes to give **26a** (0.255 g, 49%): ^1H NMR (400 MHz, CDCl_3) δ 7.92 (d, $J = 9.2$ Hz, 1H), 7.60 (s, 1H), 7.16 (s, 1H), 7.08 (t, $J = 5.5$ Hz, 1H), 6.87 (s, 1H), 6.47 (dd, $J = 2.4, 9.2$ Hz, 1H), 6.40 (d, $J = 2.4$ Hz, 1H), 4.04–3.98 (m, 2H), 3.06–3.01 (m, 2H), 2.47 (s, 3H), 1.98–1.91 (m, 2H) ppm; ^{13}C NMR (100 MHz, CDCl_3) δ 153.9, 138.0, 136.9, 129.2, 128.7, 120.0, 114.1, 110.3, 44.2, 30.5, 22.9 ppm.

N⁴-[3-(1H-Imidazol-1-yl)propyl]-2-methyl-1,4-benzenediamine (27a): A mixture of **26a** (0.233 g, 0.90 mmol) and 10% Pd/C in MeOH (20 mL) was stirred at room temperature under 52 psi of hydrogen gas for 1 h. The reaction mixture was filtered through Celite and concentrated in vacuo to give **27a** (0.166, 80%): ^1H NMR (400 MHz, CDCl_3) δ 7.48 (s, 1H), 7.07 (s, 1H), 6.92 (s, 1H), 6.58 (d, $J = 8.2$ Hz, 1H), 6.40 (d, $J = 2.6$ Hz, 1H), 6.36 (dd, $J = 2.6, 8.2$ Hz, 1H), 4.08 (t, $J = 6.9$ Hz, 2H), 3.49–3.48 (m, 1H), 3.26 (br s, 2H), 3.08–3.05 (m, 2H), 2.13 (s, 3H), 2.08–2.02 (m, 2H) ppm; ^{13}C NMR (100 MHz, CDCl_3) δ 140.9, 137.2, 136.6, 129.7, 124.3, 118.9, 116.6, 116.4, 112.3, 44.5, 41.9, 31.1, 17.7 ppm.

N-(3-Methyl-4-nitrophenyl)acrylamide (29): A mixture of 3-methyl-4-nitroaniline (**28**) (1.052 g, 6.91 mmol) and triethylamine (1.16 mL, 8.29 mmol) in CH_2Cl_2 (20 mL) was cooled to 0 °C and acryloyl chloride (0.62 mL, 7.61 mmol) was added dropwise over 5 min. The resulting mixture was stirred 1.5 h at 0 °C and then diluted with CH_2Cl_2 (35 mL), washed with brine, dried over MgSO_4 , filtered, and concentrated in vacuo to give **29** (1.941 g), which was used without further purification: MS (ES-) m/z 205.3 (M – H); ^1H NMR (400 MHz, CDCl_3) δ 8.52 (br s, 1H), 8.01 (d, $J = 9.0$ Hz, 1H), 7.75 (d, $J = 2.3$ Hz, 1H), 7.65 (dd, $J = 2.3, 9.0$ Hz, 1H), 6.49–6.40 (m, 2H), 5.78 (dd, $J = 3.4, 8.1$ Hz, 1H), 2.60 (s, 3H) ppm.

N-(3-Methyl-4-nitrophenyl)-3-(4-morpholinyl)propanamide (30): A mixture of **29** (6.91 mmol) and morpholine (0.63 mL, 7.26 mmol) in EtOH (25 mL) was warmed to reflux for 2.3 h. The reaction mixture was then concentrated in vacuo, suspended in EtOAc, and filtered. The filtrate was concentrated in vacuo, dissolved in EtOAc, and allowed to crystallize. The crystalline impurity was removed by filtration, and the filtrate was concentrated in vacuo to give **30** (1.767 g, 87%): ^1H NMR (400 Mz, CDCl_3) δ 11.24 (br s, 1H), 8.03 (d, $J = 8.9$ Hz, 1H), 7.54 (d, $J = 2.3$ Hz, 1H), 7.43 (dd, $J = 2.3, 8.9$ Hz, 1H), 3.84–3.82 (m, 4H), 2.76–2.73 (m, 2H), 2.64 (br s, 4H), 2.62 (s, 3H), 2.58–2.55 (m, 2H) ppm.

N-(4-Amino-3-methylphenyl)-3-(4-morpholinyl)propanamide (31): A mixture of **30** (0.202 g, 0.69 mmol) and 10% Pd/C (0.018 g) in MeOH (10 mL) was stirred at room temperature under 53 psi of hydrogen gas for 2.17 h. The reaction mixture was then filtered through Celite and concentrated in vacuo to give **31** (0.192 g, quant.): ^1H NMR (400 MHz, CDCl_3) δ 10.44 (br s, 1H), 7.38 (d, $J = 2.5$ Hz, 1H), 7.27 (dd, $J = 2.5, 8.3$ Hz, 1H), 6.76 (d, $J = 8.3$ Hz, 1H), 3.97–3.92 (m, 4H), 2.91–2.83 (m, 2H), 2.77–2.72 (m, 4H), 2.66–2.62 (m, 2H), 2.25 (s, 3H) ppm.

3-(3-Methyl-4-nitrophenoxy)propylamine (33): 3-Methyl-4-nitrophenol (**32**) (5.0 g, 33 mmol), 3-bromopropyl phthalimide (8.8 g, 33 mmol), and Cs_2CO_3 (16.1 g, 5.0 mmol) in DMF (60 mL) were heated to 55 °C for 2 h and then cooled to room temperature. The mixture was poured into a mixture of Et₂O and water, and the

resulting mixture was filtered, washed with water and Et₂O, and dried in a vacuum oven at 45 °C for 16 h to give 2-[3-(3-methyl-4-nitrophenoxy)propyl]-1*H*-isoindole-1,3(2*H*)-dione (**94**) (9.5 g, 85%) as a tan solid: ¹H NMR (300 MHz, DMSO-*d*₆) δ 8.05–8.01 (m, 1H), 7.90–7.84 (m, 4H), 6.88–6.85 (m, 2H), 4.16 (t, *J* = 5.8 Hz, 2H), 3.79 (t, *J* = 6.6 Hz, 2H), 2.51 (s, 3H), 2.15–2.07 (m, 2H) ppm. A solution of **94** (3.0 g, 8.8 mmol) and hydrazine hydrate (1.6 mL, 53 mmol) in EtOH (50 mL) was heated to reflux for 4 h and then stirred at room temperature for 48 h. The reaction mixture was then filtered and concentrated in vacuo. The resulting solid was washed with CH₂Cl₂ and then dissolved in EtOAc. The EtOAc solution was washed with water, dried over MgSO₄, filtered, and concentrated in vacuo to give **33** (1.1 g, 59%) as a yellow oil: ¹H NMR (400 MHz, DMSO-*d*₆) δ 7.99 (d, *J* = 9.2 Hz, 1H), 6.97 (d, *J* = 2.8 Hz, 1H), 6.91 (dd, *J* = 2.8, 9.1 Hz, 1H), 4.10 (t, *J* = 6.4 Hz, 2H), 2.63 (t, *J* = 6.7 Hz, 2H), 2.49 (s, 3H), 1.77–1.71 (m, 2H) ppm; ¹³C NMR (100 MHz, DMSO-*d*₆) δ 163.1, 142.1, 137.1, 128.0, 118.5, 113.5, 67.1, 38.8, 33.1, 21.4 ppm.

N-[3-(3-Methyl-4-nitrophenoxy)propyl]urea (**34**): A solution of **33** (0.3 g, 1.43 mmol) and trimethylsilyl isocyanate (0.21 mL, 0.18 mmol) in THF (5 mL) was stirred at room temperature for 3 h. The reaction mixture was then quenched with water (1 mL) and concentrated in vacuo. The resulting residue was washed with a mixture of EtOAc and Et₂O, filtered, and dried to afford **34** (0.273 g, 75%) as a pale yellow solid: ¹H NMR (400 MHz, DMSO-*d*₆) δ 8.00 (d, *J* = 9.2 Hz, 1H), 6.97 (d, *J* = 2.5 Hz, 1H), 6.90 (dd, *J* = 2.8, 9.1 Hz, 1H), 5.97 (t, *J* = 5.6 Hz, 2H), 5.35 (br s, 2H), 4.04 (t, *J* = 6.4 Hz, 2H), 3.08–3.03 (m, 2H), 2.44 (s, 3H), 1.81–1.74 (m, 2H) ppm.

N-[3-(4-Amino-3-methylphenoxy)propyl]urea (**35**): Compound **35** (0.045 g, 92%) was prepared from **34** according to the procedure described above for **27a**: ¹H NMR (400 MHz, DMSO-*d*₆) δ 6.51 (s, 1H), 6.48–6.43 (m, 2H), 5.92 (t, *J* = 5.6 Hz, 1H), 5.33 (br s, 2H), 4.30 (br s, 2H), 3.75 (t, *J* = 6.3 Hz, 2H), 3.08–3.03 (m, 2H), 1.96 (s, 3H), 1.70–1.64 (m, 2H) ppm.

Sodium 4-(dibenzylamino)-3-methylbenzenesulfonate (37): Mixture of 2-aminotoluene-5-sulfonic acid (10 g, 53 mmol), Na₂CO₃ (22.3 g, 210 mmol), benzyl bromide (14.3 mL, 120 mmol), water (120 mL), and CH₂Cl₂ (120 mL) was heated to reflux for 72 h. Reaction was quenched with EtOH, and the mixture was concentrated in vacuo to give 27.4 g of crude **37**, which was used without further purification.

4-(Dibenzylamino)-3-methylbenzenesulfonyl chloride (38): A solution of **37** (20.6 g, 53 mmol) in DMF (200 mL) was cooled to 0 °C, and thionyl chloride (19.0 g, 160 mmol) was added dropwise. After stirring for 2 h at room temperature, the reaction mixture was poured into ice, stirred for 30 min, and extracted with EtOAc. The organic layers were then dried over Na₂SO₄, filtered, and concentrated in vacuo to give **38** (5.0 g, 24%), which was used immediately without further purification or characterization.

4-(Dibenzylamino)-*N,N*,3-trimethylbenzenesulfonamide (39): Intermediate **38** (5.0 g, 13 mmol) was added slowly to a solution of dimethylamine (11.6 mL of 5.6M solution in EtOH, 65 mmol) at 0 °C, and the resulting mixture was stirred for 30 min at 0 °C. The reaction mixture was then poured into EtOAc and water, and the organic layer was separated, washed with brine, dried over MgSO₄, filtered, and concentrated in vacuo to give **39** (1.0 g, 20%): ¹H NMR (400 MHz, DMSO-*d*₆) δ 7.47 (d, *J* = 2.2 Hz, 1H), 7.31–7.14 (m, 11H), 7.05 (d, *J* = 8.6 Hz, 1H), 4.13 (s, 4H), 2.48 (s, 6H), 2.44 (s, 3H) ppm.

4-Amino-*N,N*,3-trimethylbenzenesulfonamide (40): A mixture of **39** (0.330 g, 0.85 mmol), toluene (10 mL), and 10% Pd/C (0.050 g) was stirred under 40 psi of H₂ gas for 6 h. The reaction mixture was then filtered through Celite, and the filtrate was washed with satd NaHCO₃ (aq) and water. The organic layer was separated, dried over MgSO₄, filtered, and concentrated in vacuo to give **40** (0.120 g, 67%): ¹H NMR (400 MHz, DMSO-*d*₆) δ 7.21–7.18 (m, 2H), 6.64 (d, *J* = 8.0 Hz, 1H), 5.74 (br s, 2H), 2.44 (s, 6H), 2.04 (s, 3H) ppm.

6-Methyl-5-nitro-2-pyridinethiol (44): Thiourea (0.2 g, 2.6 mmol) was added to a solution of **43** (0.4 g, 2.4 mmol) in ethanol

(30 mL), and the mixture was heated to reflux for 7 h. A solution of KOH (0.2 g, 3.6 mmol) in water (1 mL) was added to the reaction mixture, which was then heated for an additional 1 h. The reaction was diluted with 1 N NaOH (25 mL) and extracted with three 25-mL portions of CH₂Cl₂. The pH of the aqueous layer was then adjusted to 4 with concentrated HCl to precipitate **44** (0.124 g, 30%): LCMS (APCI+) *m/z* 171 (M + H); ¹H NMR (400 MHz, DMSO-*d*₆) δ 7.92 (d, *J* = 9.5 Hz, 1H), 7.14 (d, *J* = 9.5 Hz, 1H), 2.67 (s, 3H) ppm.

6-Methyl-5-nitro-2-pyridinesulfonamide (45): A mixture of **44** (0.115 g, 0.67 mmol) in 1 N HCl (5 mL) was cooled to 5 °C. Chlorine gas was passed through the mixture for 30 min, and the reaction was then stirred an additional 15 min. The reaction mixture was extracted with two 5-mL portions of CH₂Cl₂. The combined organic layers were cooled to 0 °C and NH₃ (l) was dripped into the mixture for 15 min via condensation of NH₃ (g) on a –78 °C coldfinger. The reaction was allowed to warm to room temperature and stir overnight. The crude mixture was concentrated in vacuo, and the residue was dissolved in EtOAc (15 mL), washed with NaHCO₃ (15 mL), dried over MgSO₄, filtered, and concentrated in vacuo to give **45** (0.06 g, 40%): GCMS (CI+) *m/z* 218 (M + H); ¹H NMR (400 MHz, DMSO-*d*₆) δ 8.60 (d, *J* = 8.4 Hz, 1H), 7.94 (d, *J* = 8.5 Hz, 1H), 7.71 (br s, 2H), 2.75 (s, 3H) ppm.

5-Amino-6-methyl-2-pyridinesulfonamide (46): A mixture of **45** (0.06 g, 0.27 mmol) and 10% Pd/C (0.011 g) in EtOH (10 mL) was stirred under H₂ (g) overnight. The reaction mixture was filtered and concentrated in vacuo to give **46**, which was used without further characterization or purification.

6-Amino-5-methyl-3-pyridinesulfonic acid (71): 3-Methyl-2-pyridineamine (1 mL, 1 mmol) was heated to 160 °C in 20% fuming sulfuric acid (2 mL) for 20 h. The reaction was then allowed to cool to room temperature, and ice (ca. 10 mL) was added. Filtration of the precipitate yielded **71** (0.094 g, 50%): ¹H NMR (300 MHz, DMSO-*d*₆) δ 13 (br s, 1H), 7.88 (s, 4H), 2.14 (s, 3H) ppm; ¹H NMR (300 MHz, DMSO-*d*₆ with D₂O) δ 7.88 (s, 2H), 7.87 (s, 2H), 2.13 (s, 3H) ppm; LCMS (ES+) *m/z* 189.

6-[(*E*)-(Dimethylamino)methylidene]amino-5-methyl-3-pyridinesulfonic acid (48): Thionyl chloride (0.5 mL, 6.8 mmol) was added to a mixture of **71** (0.9 g, 4.8 mmol) and DMF (30 mL), and the resulting mixture was stirred at room temperature for 40 min. The reaction mixture was filtered to obtain a solid, which was washed with hexane to give **48** (0.85 g, 77%): ¹H NMR (400 MHz, DMSO-*d*₆) δ 8.12 (d, *J* = 2.2 Hz, 1H), 7.50 (s, 1H), 7.00 (s, 2H), 6.47 (s, 2H), 2.02 (s, 3H) ppm; LCMS (ES+) *m/z* 244 (M + H).

6-Amino-5-methyl-3-pyridinesulfonamide (49): A mixture of **48** (1.0 g, 4.1 mmol) and PCl₅ (0.85 g, 4.1 mmol) was heated to 130 °C for 1.5 h. The resultant POCl₃ was removed under high vacuum. Concentrated NH₄OH (25 mL) was carefully added at room temperature, and the resulting mixture was heated to reflux for 4 h and then allowed to stand at room temperature for 60 h. Filtration gave **49** (0.35 g, 45%): ¹H NMR (400 MHz, DMSO-*d*₆) δ 8.12 (d, *J* = 2.4 Hz, 1H), 7.50 (d, *J* = 2.3 Hz, 1H), 7.00 (br s, 2H), 6.47 (br s, 2H), 2.02 (s, 3H) ppm; LCMS (ES+) *m/z* 188 (M + H).

1,3-Dibromo-5-chlorobenzene (51a): A solution of 1,3,5-tribromobenzene (**50**) (1.57 g, 5 mmol) in Et₂O (25 mL) was cooled to –78 °C, and *n*-BuLi (3.4 mL of 1.6 M solution in hexanes, 5.5 mmol) was added dropwise over 5 min. The reaction mixture was stirred for 10 min, and then a mixture of Cl₃CCl₃ (1.18 g, 5 mmol) in Et₂O (10 mL) was added dropwise over 3 min. The reaction mixture was stirred for 15 min at –78 °C and then allowed to warm to room temperature over 1 h. The reaction mixture was poured into water (50 mL) and extracted with two 50-mL portions of EtOAc. The combined organic layers were then dried over MgSO₄, filtered, and concentrated in vacuo to give **51a** as a yellow solid (1.24 g, 92%): ¹H NMR (300 MHz, CDCl₃) δ 7.57 (t, *J* = 1.6 Hz, 1H), 7.47 (d, *J* = 1.6 Hz, 2H) ppm; ¹³C NMR (100 MHz, CDCl₃) δ 136.0, 132.8, 130.6, 123.3 ppm; Anal. (C₆H₃Br₂Cl) C, H, N.

5-Chloro-*N*,2-dimethoxy-*N*-methylbenzamide (52): Oxalyl chloride (25 mL of 2 M solution in CH₂Cl₂, 50 mmol) was added dropwise over 30 min to a mixture of 5-chloro-2-methoxybenzoic

acid (3.73 g, 20 mmol) and 1 drop of DMF in CH_2Cl_2 (100 mL). The reaction mixture was stirred at room temperature for 21 h and then concentrated to yield 5-chloro-2-methoxybenzoyl chloride (4.1 g, quant), which was used immediately. A mixture of (MeO)-MeNH-HCl (2.54 g, 26 mmol) and triethylamine (10 mL) in CHCl_3 (40 mL) was stirred at room temperature for 10 min and then cooled to 0 °C. A solution of 5-chloro-2-methoxybenzoyl chloride (4.1 g, 20 mmol) in CHCl_3 (20 mL) was added dropwise over 30 min, and the resulting mixture was stirred at 0 °C for 30 min and then allowed to warm to room temperature over 2 h. The reaction mixture was then poured into water (100 mL) and extracted with CH_2Cl_2 (100 mL). The organic layer was washed with water (100 mL) and brine, dried over MgSO_4 , filtered, and concentrated in vacuo to give **52** (4.265 g, 93%): $^1\text{H NMR}$ (400 MHz, CDCl_3) δ 7.27 (dd, $J = 2.6, 8.8$ Hz, 1H), 7.20 (s, 1H), 6.82 (d, $J = 8.8$ Hz, 1H), 3.79 (s, 3H), 3.46 (br s, 3H), 3.29 (br s, 3H) ppm.

(3-Bromo-5-chlorophenyl)(5-chloro-2-methoxyphenyl)methanone (53a): A solution of **51a** (0.270 g, 1.0 mmol) in Et_2O (5 mL) was cooled to -78 °C, and *n*-BuLi (0.7 mL of 1.6 M solution in hexanes, 1.1 mmol) was added dropwise over 2 min. The reaction mixture was stirred at -78 °C for an additional 10 min, and then **52** (0.230 g, 1.0 mmol) was added in small portions over 4 min. The reaction mixture was stirred at -78 °C for 1.25 h and then allowed to warm to room temperature and stir for 14 h. The mixture was then poured into water (25 mL) and extracted with EtOAc (25 mL) and CH_2Cl_2 (25 mL). The combined organic layers were dried over MgSO_4 , filtered, and concentrated in vacuo to give **53a** (0.351 g, 97%): MS (APCI-) m/z 357.9 (M - H); $^1\text{H NMR}$ (300 MHz, CDCl_3) δ 7.76 (app t, $J = 1.5$ Hz, 1H), 7.70 (app t, $J = 1.8$ Hz, 1H), 7.65 (app t, $J = 1.5$ Hz, 1H), 7.47 (dd, $J = 2.7, 8.9$ Hz, 1H), 7.36 (d, $J = 2.7$ Hz, 1H), 6.95 (d, $J = 8.9$ Hz, 1H), 3.72 (s, 3H) ppm; $^{13}\text{C NMR}$ (100 MHz, CDCl_3) δ 192.4, 156.1, 140.3, 135.7, 135.6, 132.7, 130.9, 129.7, 128.8, 128.5, 126.3, 123.0, 113.2, 56.2 ppm.

3-Chloro-5-(5-chloro-2-methoxybenzoyl)benzonitrile (54a): A mixture of **53a** (0.299 g, 0.83 mmol), NaCN (0.086 g, 1.76 mmol), CuI (0.028 g, 0.15 mmol), and Pd(PPh₃)₄ (0.113 g, 0.10 mmol) in acetonitrile (8 mL) was warmed to reflux for ca. 45 min. The reaction mixture was cooled to room temperature, diluted with EtOAc (50 mL), and filtered through Celite. The solution was then washed with water (25 mL), dried over MgSO_4 , filtered, and concentrated in vacuo. Column chromatography on silica gel (elution with 5% EtOAc in hexanes) gave **54a** (0.171 g, 56%): $^1\text{H NMR}$ (400 MHz, CDCl_3) δ 7.93 (app t, $J = 1.8$ Hz, 1H), 7.82 (app t, $J = 1.5$ Hz, 1H), 7.76 (app t, $J = 1.7$ Hz, 1H), 7.47 (dd, $J = 2.5, 8.9$ Hz, 1H), 7.37 (d, $J = 2.5$ Hz, 1H), 6.93 (d, $J = 8.9$ Hz, 1H), 3.67 (s, 3H) ppm; $^{13}\text{C NMR}$ (100 MHz, CDCl_3) δ 191.8, 156.2, 140.1, 135.9, 135.6, 133.6, 133.3, 1314, 130.0, 128.0, 126.7, 116.9, 114.4, 113.3, 56.1 ppm.

3-Chloro-5-(5-chloro-2-hydroxybenzoyl)benzonitrile (55a): Prepared from **54a** according to the procedure described above for **7**. Isolated **55a** (0.174 g, quant) as a yellow solid: $^1\text{H NMR}$ (400 MHz, CDCl_3) δ 11.43 (s, 1H), 7.84–7.82 (m, 2H), 7.78 (t, $J = 1.5$ Hz, 1H), 7.49 (dd, $J = 2.7, 9.0$ Hz, 1H), 7.34 (d, $J = 2.7$ Hz, 1H), 7.05 (d, $J = 9.0$ Hz, 1H) ppm; $^{13}\text{C NMR}$ (100 MHz, CDCl_3) δ 196.9, 162.1, 139.9, 137.7, 136.3, 135.1, 133.2, 131.6, 130.5, 124.4, 120.9, 118.9, 116.6, 114.8 ppm.

(2-Bromophenyl)(5-chloro-2-hydroxyphenyl)methanone (61a): A mixture of 2-bromobenzoyl chloride (10 g, 46 mmol), aluminum chloride (6.2 g, 46 mmol), and 4-chloroanisole (5.6 mL, 46 mmol) in CH_2Cl_2 (250 mL) was stirred at reflux overnight. The reaction mixture was then cooled to room temperature, poured into ice-water, and extracted with CH_2Cl_2 . The organic layer was dried over MgSO_4 , filtered, and concentrated in vacuo to give **61a** (13.76 g, 96%) as a tan solid: $^1\text{H NMR}$ (400 MHz, $\text{DMSO}-d_6$) δ 10.92 (s, 1H), 7.70 (d, $J = 7.9$ Hz, 1H), 7.49–7.42 (m, 3H), 7.54 (dd, $J = 2.7, 9.0$ Hz, 1H), 7.29 (d, $J = 2.8$ Hz, 1H), 6.98 (d, $J = 9.0$ Hz, 1H) ppm.

{2-[(2-Bromophenyl)carbonyl]-4-chlorophenyl}oxy}acetic acid (63a): Intermediate **61a** was converted in two steps to **63a** (17.24 g, 98%) according to the procedures described above for conversion

of **7** to **9**: $^1\text{H NMR}$ (400 MHz, $\text{DMSO}-d_6$) δ 12.96 (br s, 1H), 7.67–7.64 (m, 1H), 7.59 (dd, $J = 2.8, 9.0$ Hz, 1H), 7.49 (d, $J = 2.8$ Hz, 1H), 7.43–7.38 (m, 3H), 7.07 (d, $J = 9.0$ Hz, 1H), 4.49 (s, 2H) ppm.

2-[(2-[(2-Bromophenyl)carbonyl]-4-chlorophenyl)oxy]-N-[2-methyl-4-(1-oxido-4-thiomorpholinyl)phenyl]acetamide (65a): A mixture of **63a** (0.443 g, 1.2 mmol), 1-hydroxybenzotriazole (0.16 g, 1.2 mmol), 1-(3-dimethylaminopropyl)-3-ethylcarbodiimide hydrochloride (0.23 g, 1.2 mmol), triethylamine (0.34 mL, 2.4 mmol) and aniline **64** (0.40 g, 1.8 mmol) in DMF (15 mL) was stirred at room-temperature overnight. The reaction mixture was then partitioned between EtOAc and water. The organic layer was separated, washed with water and brine, dried over MgSO_4 , filtered, and concentrated in vacuo. Column chromatography on silica gel (elution with 2% MeOH/ CH_2Cl_2) gave **65a** (0.154 g, 22%) as an off-white foam: $^1\text{H NMR}$ (400 MHz, $\text{DMSO}-d_6$) δ 8.80 (s, 1H), 7.70–7.64 (m, 2H), 7.50–7.36 (m, 4H), 7.24 (d, $J = 8.8$ Hz, 1H), 7.15 (d, $J = 8.8$ Hz, 1H), 6.85 (d, $J = 2.6$ Hz, 1H), 6.79 (dd, $J = 3, 8$ Hz, 1H), 4.62 (s, 2H), 3.73–3.67 (m, 2H), 3.56–3.51 (m, 2H), 2.91–2.84 (m, 2H), 2.67–2.61 (m, 2H), 2.07 (s, 3H) ppm.

2-[4-Chloro-2-(2-cyanobenzoyl)phenoxy]-N-[2-methyl-4-(1-oxido-4-thiomorpholinyl)phenyl]acetamide (66a): Copper cyanide (0.037 g, 0.42 mmol) was added to a solution of **65a** (0.120 g, 0.21 mmol) in DMF (5 mL), and the resulting mixture was heated to 160 °C and stirred overnight. The mixture was then cooled, and water was added. The resulting solid was filtered and washed with EtOAc. The filtrate was dried over MgSO_4 and concentrated in vacuo. Column chromatography on silica gel (elution with 10–100% EtOAc/hexanes) gave **66a** (0.012 g, 11%) as an orange foam: $^1\text{H NMR}$ (400 MHz, $\text{DMSO}-d_6$) δ 8.97 (s, 1H), 7.99–7.96 (m, 1H), 7.76–7.66 (m, 4H), 7.56 (d, $J = 2.7$ Hz, 1H), 7.22 (d, $J = 8.9$ Hz, 1H), 7.06 (d, $J = 8.6$ Hz, 1H), 6.82 (d, $J = 3.0$ Hz, 1H), 6.76 (dd, $J = 3, 9$ Hz, 1H), 4.62 (s, 2H), 3.73–3.69 (m, 2H), 3.55–3.53 (m, 2H), 2.90–2.84 (m, 2H), 2.65–2.60 (m, 2H), 1.99 (s, 3H) ppm; MS (ES-) m/z 521 (M - H); Anal. ($\text{C}_{27}\text{H}_{24}\text{N}_3\text{O}_4\text{ClS} + 0.3 \text{ H}_2\text{O}$) C, H, N, S.

[3,5-Bis(methoxy)phenyl](5-chloro-2-hydroxyphenyl)methanone (69a): A solution of 2-bromo-4-chlorophenol (0.830 g, 4.0 mmol) in THF (20 mL) was cooled to -78 °C. *n*-Butyllithium (5.5 mL of a 16 M solution in hexanes, 8.8 mmol) was added dropwise over 5 min, and the resulting mixture was stirred at -78 °C for 1 h. A solution of **68** (0.901 g, 4.0 mmol) in THF (5 mL) was added dropwise over 4 min, and the resulting mixture was stirred at -78 °C for 1.25 h and then at room temperature for 14 h. The reaction mixture was poured into water (50 mL) and extracted with two 50-mL portions of EtOAc. The combined organic layers were dried over MgSO_4 , filtered, and concentrated in vacuo to give 1.193 g of a brown oil. Column chromatography on silica gel (elution with 10% EtOAc/hexanes), followed by crystallization from hot ether gave **69a** (0.234 g, 20%) as yellow crystals: $^1\text{H NMR}$ (300 MHz, CDCl_3) δ 11.83 (s, 1H), 7.62 (d, $J = 2.6$ Hz, 1H), 7.45 (dd, $J = 2.6, 8.9$ Hz, 1H), 7.03 (d, $J = 8.9$ Hz, 1H), 6.76 (d, $J = 2.3$ Hz, 2H), 6.68 (t, $J = 2.3$ Hz, 1H), 3.84 (s, 6H) ppm; $^{13}\text{C NMR}$ (100 MHz, CDCl_3) δ 200.6, 161.9, 160.9, 139.1, 136.5, 132.6, 123.6, 120.2, 119.9, 107.1, 104.5, 55.9 ppm; Anal. ($\text{C}_{15}\text{H}_{13}\text{O}_4\text{Cl}$) C, H, N.

N-[4-(Aminosulfonyl)-2-methylphenyl]-2-[4-chloro-2-(3-chloro-5-cyanobenzoyl)phenoxy]acetamide (70h): Prepared from **55a** and **21b** according to the procedure described above for **24a**. Column chromatography on silica gel (elution with 0.5–1% MeOH/ CH_2Cl_2) gave **70h** (0.033 g, 12%) as a light yellow solid: $^1\text{H NMR}$ (400 MHz, $\text{DMSO}-d_6$) δ 9.42 (s, 1H), 8.26 (s, 1H), 8.11 (s, 1H), 8.03 (t, $J = 1.6$ Hz, 1H), 7.63 (dd, $J = 2.7, 8.9$ Hz, 1H), 7.60–7.53 (m, 3H), 7.49 (d, $J = 2.7$ Hz, 1H), 7.22 (s, 2H), 7.19 (d, $J = 9.1$ Hz, 1H), 4.77 (s, 2H), 2.14 (s, 3H), ppm; $^{13}\text{C NMR}$ (100 MHz, $\text{DMSO}-d_6$) δ 192.0, 166.6, 155.2, 141.0, 139.9, 139.1, 136.7, 135.1, 133.8, 133.4, 132.7, 131.9, 130.1, 128.6, 128.3, 126.0, 124.5, 124.3, 117.5, 116.0, 114.3, 67.7, 18.4 ppm; MS (APCI-) m/z 517 (M - H); Anal. ($\text{C}_{23}\text{H}_{17}\text{N}_3\text{O}_5\text{Cl}_2\text{S}$) C, H, N.

Activity against HIV-1 in an Acute Infection Assay Using MT4 Cells. The human T-cell lymphotropic virus type-1 trans-

formed cell line MT4 was infected with HIV-1 (strain IIIB) at 100 times the amount necessary to cause a 50% reduction in cell growth. The infected cells were incubated for 5 days in the presence of various concentrations of each of the compounds to be tested. HIV-1-mediated cytopathic effects (CPE) were assessed by an MTS Staining method. A compound that expresses activity against HIV-1 prevents this CPE. Each value represents the mean from a single experiment performed in triplicate. Compound induced cytotoxicity was measured in parallel in uninfected cells (data not shown). For the benzophenone compound series, cytotoxicity was not observed up to 0.5 μ M, which was, in most cases, the highest concentration tested.

HeLa MAGI Assay. The assay used in this report is a modified version of the HeLa MAGI system¹⁴ in which HIV-1 infection is detected by the activation of an HIV-LTR driven β -galactosidase reporter in HeLa CD4-LTR- β -gal cells (obtained from Dr. Michael Emerman through the AIDS Research and Reference Reagent Program, Division of AIDS, NIAID, NIH). Quantitation of β -galactosidase is achieved by measuring the activation of a chemiluminescent substrate (Tropix/Applied Biosystems, Foster City, CA) 3 days after infection. The concentration of each compound required to inhibit 50% (IC_{50}) of the HIV-1-induced β -galactosidase signal, relative to untreated controls was determined for each isogenic recombinant virus. Cytotoxicity was measured in parallel using the CellTiter96 assay (Promega, Madison, WI) to ensure that the loss of signal was in fact due to a reduction in HIV replication and not cytotoxicity (data not shown). For the benzophenone compound series, cytotoxicity was not observed up to 0.5 μ M, which was, in most cases, the highest concentration tested.

Virus Strains: HIV-1 strain IIIB was derived from cell-free supernatants of cultures of the chronically infected cell line H93B (H9/HTLV-IIIB). The nevirapine-resistant strain designated Nev-R contains the Y181C mutation in RT. HIV-1 strain HxB2 was derived from the molecular clone pHxB2-D.¹⁵ Construction of recombinant DNA-derived isogenic strains containing wild type (WT) RT or NNRTI-resistant mutations K103N, V106A, or Y181C is described in ref 10.

Pharmacokinetic Studies. Compounds **70g** and **70h** (GW678248) were each dissolved in PEG400:Solutol:H₂O (30:20:50) at 0.5 mg/mL and administered intravenously via bolus infusion at 1 mg/kg (2 mL/kg) to male Han Wistar rats, beagle dogs, and cynomolgus monkeys (two animals per species per compound). Blood samples were collected in EDTA-containing tubes prior to dosing and at selected times up to 24 h post-dose from each animal. The samples were kept on ice until centrifuged to obtain plasma (typically within 30 min of collection), and the resulting plasma samples were stored at or below -20 °C until analyzed. Rat studies were conducted at GlaxoSmithKline (RTP, NC) in accordance with GSK Institutional Animal Care and Use Committee (IACUC) protocols and guidelines. In-life portions of the dog and monkey studies were conducted at Primedia Corporation/Charles River Laboratories (Worcester, MA) under their IACUC-approved protocols. All plasma analyses were performed at GlaxoSmithKline.

Plasma samples and calibration standards (0.1-mL aliquot) were deproteinated by addition of acetonitrile (0.3–0.4 mL) or methyl-*tert*-butyl ether (0.5 mL) followed by centrifugation (15800g, 4 °C, 5 min). The resulting supernatants were evaporated to dryness at 37 °C under nitrogen, and each dried extract was reconstituted with 20% acetonitrile in 0.1% acetic acid, pH 4.5 (0.1 mL). The plasma extracts were analyzed by HPLC/MS using a Phenomenex Aqua C18 Mercury column (3 micron; 20 \times 2 mm) and a Sciex API 365 triple-quadrupole mass spectrometer equipped with a Turbo Ion Spray source. Mobile phases were: (A) 5% acetonitrile in 0.1% acetic acid, pH 4.6, and (B) 0.1% acetic acid in neat acetonitrile. Samples (10- to 30- μ L aliquots) were eluted from the analytical column with a 1-min linear gradient from 80%A:20%B to 5%A:95%B followed by a 1-min isocratic elution with 5%A:95%B at a constant flow rate of 0.4 mL/min. The analytes were detected by negative-ion MRM, monitoring the transitions m/z 496.1 to m/z 270.0 for **70g** or m/z 516.1 to m/z 289.7 for **70h** (GW678248) at a collision energy of 35 eV. Drug concentrations in plasma were

determined by reference to a corresponding calibration curve constructed by linear or quadratic regression analysis of $1/x$ - or $1/x^2$ -weighted standard peak areas. Pharmacokinetic parameter values were estimated by noncompartmental analysis of the plasma concentration–time curves.

Acknowledgment. The authors thank Gwyer Lovell, Brian Owens and Pat Wheelan for conducting the pharmacokinetics studies and Thimysta Burnette for providing the pharmacokinetics data.

Supporting Information Available: Procedures and characterization data for **18a**, **19**, **24a,b**, **41a–d**, **42b–c**, **42e–f**, **56a,b**, **57a,b**, **58a,b**, **59**, **66b–c**, **67**, **70a–g**, **70i** and all intermediates used in the preparation of these compounds; results from combustion analyses. This material is available free of charge via the Internet at <http://pubs.acs.org>.

References

- (1) Staszewski, S.; Morales-Ramirez, J.; Tashima, K. T.; Rachlis, A.; Skiest, D.; Stanford, J.; Stryker, R.; Johnson, P.; Labriola, D. F.; Farina, D.; Manion, D. J.; Ruiz, N. M. Efavirenz plus zidovudine and lamivudine, efavirenz plus indinavir, and indinavir plus zidovudine and lamivudine in the treatment of HIV-1 infection in adults. *N. Engl. J. Med.* **1999**, *341*, 1865–1873.
- (2) Zhang, Z.; Hamatake, R.; Hong, Z. Clinical utility of current NNRTIs and perspectives of new agents in this class under development. *Antiviral Chem. Chemother.* **2004**, *15*, 121–134.
- (3) *Guidelines for the use of antiretroviral agents in HIV-1-infected adults and adolescents.* Published by the US Department of Health and Human Services. Oct 29, 2004. Available at <http://AIDSinfo.nih.gov>.
- (4) Grant, R. M.; Hecht, F. M.; Warmerdam, M.; Liu, L.; Liegler, T.; Petropoulos, C. J.; Hellmann, N. S.; Chesney, M.; Busch, M. P.; Kahn, J. O. Time trends in primary HIV-1 drug resistance among recently infected persons. *JAMA* **2002**, *288*, 181–188.
- (5) Ross, L. L.; Lim, M. L.; Liao, Q.; Wine, B.; Rodriguez, A. E.; Weinberg, W.; Shafer, M. Prevalence of antiretroviral drug resistance and resistance mutations in antiretroviral therapy (ART) naïve HIV infected individuals from 44 cities during 2003. Presented at the 44th Interscience Conference on Antimicrobial Agents and Chemotherapy Meeting, Oct. 30 – Nov. 2, 2004, Washington, DC, Abstract H-173.
- (6) Wyatt, P. G.; Bethell, R. C.; Cammack, N.; Charon, D.; Dodic, N.; Dumaitre, B.; Evans, D. N.; Green, D. V. S.; Hopewell, P. L.; Humber, D. C.; Lamont, R. B.; Orr, D. C.; Plested, S. J.; Ryan, D. M.; Sollis, S. L.; Storer, R.; Weingarten, G. G. Benzophenone derivatives: A novel series of potent and selective inhibitors of human immunodeficiency virus type 1 reverse transcriptase. *J. Med. Chem.* **1995**, *38*, 1657–1665.
- (7) Chan, J. H.; Freeman, G. A.; Tidwell, J. H.; Romines, K. R.; Schaller, L. T.; Cowan, J. R.; Gonzales, S. S.; Lowell, G. S.; Andrews, C. W.; Reynolds, D. J.; St. Clair, M.; Hazen, R. J.; Ferris, R. G.; Creech, K. L.; Roberts, G. B.; Short, S. A.; Weaver, K.; Koszalka, G. W.; Boone, L. R. Novel benzophenones as nonnucleoside reverse transcriptase inhibitors of HIV-1. *J. Med. Chem.* **2004**, *47*, 1175–1182.
- (8) (a) Stammers, D. K.; Stuart, D. I.; Ren, J.; Chamberlain, P. P.; Weaver, K.; Short, S.; Andrews, C.; Romines, K.; Boone, L.; Schaller, L.; Freeman, A.; Chan, J. Structural studies of benzophenone/HIV-1 RT complexes: Insights into the potency of the next generation NNRTIs against wt and mutant HIV-1. Presented at the XIII International HIV Drug Resistance Workshop, June 8–12, 2004, Canary Islands, Spain, Poster 30. (b) Stammers, D. K., et al., unpublished results.
- (9) Structure–activity relationships in this manuscript were determined using HIV antiviral assays. These antiviral assays have been shown to correlate well with enzyme inhibition in biochemical assays (ref 7, footnote 10).
- (10) Ferris, R.; Hazen, R.; Roberts, G.; St. Clair, M.; Chan, J.; Romines, K.; Freeman, G.; Tidwell, J.; Schaller, L.; Cowan, J.; Short, S.; Weaver, K.; Selleseth, D.; Moniri, K.; Boone, L. Antiviral activity of GW678248, a novel benzophenone nonnucleoside reverse transcriptase inhibitor. *Antimicrob. Agents Chemother.* **2005**, *49*, 4046–4051.
- (11) 2-Bromo-1-methoxy-4-(trifluoromethyl)benzene was obtained by O-methylation of trifluoro-*p*-cresol using methyl iodide and potassium carbonate in acetone, followed by bromination using bromine and sodium acetate in acetic acid.

- (12) The chloro starting material **43** was not commercially available, so we prepared it in two steps from 6-methyl-2-pyridineamine. The 3-nitro group was installed using sulfuric and fuming nitric acids, and the amine was converted to a chloro group using trimethylsilyl chloride and *tert*-butyl nitrite.
- (13) Kamm, O. β -Phenylhydroxylamine. *Organic Syntheses Collective Volume I*; Blatt, A. H., Ed.; John Wiley & Sons: New York, 1932; pp 445–447.
- (14) Kimpton, J.; Emerman, M. Detection of Replication-competent and Pseudotyped Human Immunodeficiency Virus with a Sensitive Cell Line on the Basis of Activation of an Integrated β -galactosidase Gene. *J. Virol.* **1992**, *66*, 2232–2239.
- (15) Fisher, A. G.; Collati, E.; Ratner, L.; Gallo, R. C.; Wong-Stall, F. A molecular clone of HTLV-III with biological activity. *Nature* **1985**, *316*, 262–265.

JM050670L